ATSC Recommended Practice: A/327:2025-02 Amendment No. 1, "MIMO System Performance Estimation"

Doc. A/327:2025-02 Amend. No. 1
26 June 2025

Advanced Television Systems Committee
1300 I Street, N.W., Suite 400E
Washington, D.C. 20005
202-872-9160

Implementers with feedback, comments, or potential bug reports relating to this document may contact ATSC at https://www.atsc.org/feedback/.

Revision History

Version	Date
Amendment approved	26 June 2025

ATSC Recommended Practice: A/327:2025-02 Amendment No. 1, “MIMO System Performance Estimation”

1. OVERVIEW

1.1 Definition

An Amendment is generated to document an enhancement, an addition or a deletion of functionality to previously agreed technical provisions in an existing ATSC document. Amendments shall be published as attachments to the original ATSC document. Distribution by ATSC of existing documents shall include any approved Amendments.

1.2 Scope

This amendment aligns with New Project Proposal N-074, “ATSC 3.0 MIMO Extension,” and provides reference information for ATSC 3.0 MIMO practices. It describes methods estimating ATSC 3.0 MIMO system performance, which governs the physical coverage of MIMO broadcast networks. The underlying channel modeling and characterization supporting the presented methods are also described.

1.3 Rationale for Changes

ATSC A/322 defined optional technologies MIMO and Layered MIMO to enhance capacity and improve spectral efficiency. Despite this system design, ATSC A/327 lacks rationale data or methodologies for estimating network coverage and signal robustness when using MIMO. Providing practical means to estimate the physical layer performance of ATSC 3.0 MIMO systems and characterize the associated channel conditions will benefit the industry.

1.4 Compatibility Considerations

The changes described in this document are backward compatible with the currently published version of the standard to which this Amendment pertains and any previously approved Amendments for that standard. Guidance provided in this amendment is limited to system performance prediction and does not affect any receiver’s ability.

2. LIST OF CHANGES

Change instructions are given below in *italics*. Unless otherwise noted, inserted text, tables, and drawings are shown in blue; deletions of existing text are shown in ~~red~~. The text “[ref]” indicates that a cross reference to a cited referenced document should be inserted. Yellow highlighted references indicate the document editor should insert the appropriate internal document references.

2.1 Change Instructions

Add one new item to Section 2, “References.”

[19] ATSC: “ATSC Standard: ATSC 3.0 MIMO Extension,” Doc. A/322:2024-04 Amendment No. 1, Advanced Television System Committee, Washington, D.C., 13 September 2024.

Add three new items to Section 3.2, “Acronyms and Abbreviations.”

CSI Channel State Information

CSIR CSI at the Receiver
PHY PHYsical layer
XPD Cross-Polarization Discrimination

Add two new items to Section 3.3, "Terms."

Cross-Polarization Discrimination (XPD) – The ratio of the power in a co-polarized wave to the power in a cross-polarized wave.

PHY Functional Scalability – An attribute pertaining to SISO, MIMO, channel bonding, and their combined operations, describing the hierarchical compatibility among these technology sets (see Section 4.2.22).

Modify Section 4.2.21, "MIMO Operation," as follows:

4.2.21 MIMO Operation

MIMO (Multiple Input Multiple Output) in ATSC 3.0 allows a higher spectral efficiency and/or a higher transmission robustness compared to SISO via additional spatial diversity and multiplexing by sending two data streams in a single radio frequency channel. Although it is not directly specified in the physical layer protocol standard [3], it is expected in practice to use cross-polarized 2×2 MIMO (i.e., horizontal and vertical polarization) to retain multiplexing capabilities in line-of-sight conditions.

The MIMO operation is indicated and optionally enabled on a per subframe basis (via **L1B_first_sub_mimo** and/or **L1D_mimo**) within an ATSC 3.0 transmission. All MIMO-enabled subframes within the same ATSC 3.0 physical layer frame must use the same MIMO pilot encoding scheme, since this scheme is indicated only on a per frame basis (via **L1B_mimo_scattered_pilot_encoding**).

In [3], two MIMO pilot antenna encoding schemes, Walsh-Hadamard encoding and Null Pilot encoding, have been defined and one of these two schemes is selected to be configured for use within a transmitted ATSC 3.0 waveform for 2×2 MIMO channel estimation. The two MIMO pilot encoding schemes are configured with the same pilot positions and boosting as SISO pilots, which are described in Section 4.2.3 and 4.2.4. It is recommended that the configured MIMO pilot encoding scheme be selected according to intended service scenarios and receiver implementations. For a fixed reception scenario in a time-invariant channel, it is recommended to use the Null Pilot encoding scheme since the 3 dB boosting in pilot power improves channel estimation accuracy at a receiver. For a mobile reception scenario in a high Doppler time-varying channel, it is recommended to use the Walsh-Hadamard encoding scheme for MIMO pilots because of the higher Doppler shift limit for frequency channel variation f_D described in Section 4.2.3.2.

4.2.21.1 Layered MIMO Operation

LDM can be applied to multiplex a MIMO PLP with other PLPs, and the procedures for doing so are specified in Annex O of [3]. The combination of LDM and MIMO is referred to in [3] as Layered MIMO.

ATSC 3.0 defines two types of Layered MIMO operations, namely, Layered MIMO Type A and Layered MIMO Type B. Type A is a homogeneous superposition of MIMO PLPs, whereas Type B combines a SISO Core PLP and a MIMO Enhanced PLP. These designs attribute extensive throughput to Type A and versatile backward compatibility to Type B.

The use and type of Layered MIMO are indicated on a subframe basis. **L1D_mimo** (or **L1B_first_sub_mimo**), **L1D_mimo_mixed** (or **L1B_first_sub_mimo_mixed**), and **L1D_plp_layer** participate in this indication, as specified in Sections 9.2.3, 9.3.3, and O.14 of [3]. The enabling of **L1D_mimo** and **L1D_mimo_mixed** is mutually exclusive (see Tables 9.8 and 9.10 of [3]). This design is a measure to ensure backward compatibility with existing SISO receivers when Layered MIMO Type B is applied. **L1D_mimo_mixed** identifies whether the corresponding subframe includes a heterogeneous mixture of SISO and MIMO PLPs. Nevertheless, ATSC 3.0 SISO receivers fielded before the release of [19] may be unable to parse **L1D_mimo_mixed** (or **L1B_first_sub_mimo_mixed**) because this signaling field was not defined until [19]. Accordingly, the existing SISO receivers can ignore the PLPs indicated by **L1D_mimo** (or **L1B_first_sub_mimo**) =1. When Layered MIMO Type B is applied, **L1D_mimo** (or **L1B_first_sub_mimo**) =0 is set and the SISO receivers will proceed with decoding the Core PLP encoded in SISO. On the contrary, MIMO receivers manufactured after the release of [19] are available to access the combination of **L1D_mimo** (or **L1B_first_sub_mimo**) and **L1D_mimo_mixed** (or **L1B_first_sub_mimo_mixed**), and hence proceeds with decoding MIMO Enhanced PLP even while **L1D_mimo** (or **L1B_first_sub_mimo**) =0 is seen for the Layered MIMO Type B subframe.

Basically, the use of LDM in a subframe is indicated by a nonzero **L1D_plp_layer**. However, in the current version of the standard [3], **L1D_mimo_mixed** (or **L1B_first_sub_mimo_mixed**) =1 also directs the use of LDM, as only a form of Layered Type B is permitted for the mixed use of SISO and MIMO within a subframe. This means that whenever **L1D_mimo_mixed** (or **L1B_first_sub_mimo_mixed**) =1 is set, one or more PLPs holding **L1D_plp_layer** >0 shall be included in the corresponding subframe.

Within subframes using Layered MIMO Type B, MIMO and SISO PLPs are recognized by **L1D_plp_mimo**. This field is conditionally announced only when **L1D_mimo_mixed** (or **L1B_first_sub_mimo_mixed**) =1 is flagged[1]. Note that Layered MIMO Type B applies SISO to all Core PLPs and MIMO to all Enhanced PLPs. Therefore, PLPs in such subframes accompany **L1D_plp_mimo** =0 with **L1D_plp_layer** =0 and **L1D_plp_mimo** =1 with **L1D_plp_layer** >0.

Whenever both SISO and MIMO PLPs are present in a frame, MIMO PLPs employ Walsh-Hadamard pilot encoding to secure compatibility with SISO PLPs. This applies to frames containing Layered MIMO Type B subframe(s) and frames alternating between SISO and MIMO subframes. In terms of L1-signaling parameters, the condition can be expressed as follows: The presence of **L1D_mimo_mixed** (or **L1B_first_sub_mimo_mixed**) =1, or the coexistence of differing **L1D_mimo** (or **L1B_first_sub_mimo**) values. This constraint sets **L1B_mimo_scattered_pilot_encoding** =0, which applies to the entire portion of a single frame. As a result, all subframes within such frames shall use Walsh-Hadamard or SISO pilot encoding.

When MISO mode is enabled with Layered MIMO Type B, a single MIMO transmitter applies different TDCFS code indices to each Polarization. Specifically, within a **Per_Transmit_Polarization_Data()**, STLTP assigns different values of **miso_filt_code_index** to Polarizations #1 and #2. This mitigates correlated pilot contamination at SISO receivers, which may result from cross-Polarization interference under Walsh-Hadamard pilot encoding.

When Layered MIMO Type B is used, a constraint implied by the IFFT equations in Section O.12 of [3] requires that all Enhanced PLPs in the subframe apply the same injection level. In other words, if **L1D_mimo_mixed** (or **L1B_first_sub_mimo_mixed**) =1, all constituent PLPs with **L1D_plp_layer** >0 shall be configured with the same value of **L1D_plp_ldm_injection_level**. This constraint applies not only to non-aligned LDM examples in Section 7.2.7.4.3 of [3] and Section 5.3.3.3 but also to

[1] In the current version of the standard, **L1D_mimo_mixed** (or **L1B_first_sub_mimo_mixed**) =1 is exclusive to Layered MIMO Type B.

any possible configurations of Type B subframes, regardless of **L1D_plp_start** values. This ensures system simplicity and maintains a uniform signal level within a subframe.

System simplicity in Layered MIMO Type A is also achieved by constraining MIMO precoding configurations. Layered MIMO Type A involves two MIMO PLPs, each undergoing an individual MIMO precoding process configured with its own parameter set {**L1D_plp_mimo_stream_combining**, **L1D_plp_mimo_IQ_interleaving**, **L1D_plp_mimo_PH**}. However, those associated Core and Enhanced PLPs are constrained to have identical **L1D_plp_mimo_IQ_interleaving** values and identical **L1D_plp_mimo_PH** values. This means that Layered MIMO Type A applies exactly the same I/Q polarization interleaving and phase hopping operations to the Core and Enhanced PLPs, thereby allowing reduced complexity at the receiver. Unlike the rest, stream combining varies with ModCod combinations even if **L1D_plp_mimo_stream_combining** is identical. For this reason, the constraints have been introduced only to I/Q polarization interleaving and phase hopping.

According to Section 7.1.3 in [3], extended time interleaving mode is not allowed for LDM. Therefore, extended time interleaving shall not be applied to any PLPs participating in Layered MIMO even when MIMO precoding is not in use (see Sections L.6 and O.7 in [3]).

Section O.12.1 in [3] states that subframes shall be arranged in descending order of the scaling factor $K_m[1]$. Note that SISO subframes having Polarization #2 muted (i.e., the 1st option in Section L.11.2) do not define $K_m[1]$. This does not mean that $K_m[1]$ is zero for such subframes. Therefore, such SISO subframes precede Layered MIMO subframes.

4.2.21.2 Combined Operation of MIMO and Channel Bonding

MIMO and channel bonding can be jointly applied as specified in Sections K.4, L.13, and O.13 of [3]. In other words, MIMO can be applied to one or more RF channels over which data from a single PLP are spread.

The use of this combination is indicated when both technology subsets, MIMO and channel bonding, are enabled, while each is signaled independently. No new flag parameters are required for this combined use. Channel bonding is signaled by **L1D_num_rf** and **L1D_plp_num_channel_bonded**, while **L1D_mimo** (or **L1B_first_sub_mimo**), **L1D_mimo_mixed** (or **L1B_first_sub_mimo_mixed**), and **L1D_plp_mimo** signal the use of MIMO.

Note that **L1D_num_rf** and **L1D_plp_num_channel_bonded** apply on a frame and PLP basis, respectively. A nonzero **L1D_num_rf** indicates only the presence of PLP(s) engaged in channel bonding, while the specific PLP(s) participating are identified by **L1D_plp_num_channel_bonded** =1. For a PLP holding **L1D_plp_num_channel_bonded** =1 in the current RF channel, **L1D_bonded_bsid** is where to find the counterpart RF channel. **L1D_bonded_bsid** corresponds to the **L1D_bsid** of the counterpart RF channel, with the BSID assignment being regionally unique (see Sections 3.4 and 9.3.2 in [3]). A channel-bonded PLP holds an identical, unique **L1D_plp_id** across the engaged RF channels. Based on this premise, the positions of channel-bonded signals are precisely specified by tracing **L1D_plp_id** within the engaged RF channels.

Both plain and SNR averaging modes of channel bonding remain applicable even when combined with MIMO. A 2-bit parameter **L1D_plp_channel_bonding_format** determines the channel bonding mode, shortly indicating whether the cell exchange block is enabled. Behind its use, cell exchange requires tight synchronicity and PLP rate matching as a prerequisite.

As long as plain channel bonding is used (**L1D_plp_channel_bonding_format** = 00), a channel-bonded PLP can be modulated differently in each individual RF channel, and this applies to MIMO as well. This means that bonding between MIMO and SISO signals is allowed. Such configurations enable cooperation between MIMO transmitter and SISO transmitter that are not co-located. Broadcast Gateway operations running two separate STLTP tunneled data streams (defined in Section 9.5 and Annex E of [5]) support this type of channel bonding. The bonding can also be applied alongside Layered MIMO, and bonding between CL and EL signals is allowed. For example, SISO-modulated CL signals in RF channel #0 can be bonded with MIMO EL signals in RF channel #1. This allowance also includes channel bonding between LDM and non-LDM signals.

Note that MIMO-capable transmitters also support SISO operations based on their physical capability. Thus, channel bonding between MIMO and SISO paths allows SFNs to coordinate the following three types of transmitter sets: (*i*) A co-located transmitter unit that exclusively handles the combined operation of MIMO and channel bonding; (*ii*) a pair of MIMO transmitters cooperating for channel bonding, but not co-located; (*iii*) a MIMO transmitter and a SISO transmitter cooperating for channel bonding, but not co-located. This maximizes the opportunity to reuse transmitter/network resources, enabling flexible and efficient SFN construction.

Not only transmitters but also receivers supporting the combined operation of MIMO and channel bonding are also capable of individually operating in MIMO, channel bonding, and SISO modes. Receivers compatible with channel-bonded MIMO, necessarily equipped with two Polarization antenna sets, can also process the bonding of MIMO and SISO signals.

Nevertheless, the heterogeneous form of channel bonding is available only in the absence of SNR averaging mode. If SNR averaging is applied (**L1D_plp_channel_bonding_format** = 01), the channel-bonded PLP must maintain across the bonded RF channels the same configurations of: BICM setting, TI setting, number of FEC Blocks per subframe, multiplexing scheme, LDM layer index, use of MIMO, MIMO precoding setting, and Layered MIMO Type. The related L1 parameters include **L1D_mimo**, **L1D_mimo_mixed**, **L1D_plp_mimo**, **L1D_plp_layer**, **L1D_plp_mimo_stream_combining**, **L1D_plp_mimo_IQ_interleaving**, **L1D_plp_mimo_PH**, **L1D_plp_TI_mode**, **L1D_plp_CTI_depth**, **L1D_plp_size**, **L1D_plp_mod**, **L1D_plp_cod**, **L1D_plp_ldm_injection_level**, etc. That is, whenever SNR averaging is used, both partitioned streams under channel-bonded MIMO operation apply MIMO in the same way, and bonding occurs only within the same LDM layer. Additionally, cell exchange occurs only within each Polarization independently (as specified in Section L.13 of [3]).

Replace Section 4.2.22 with the following content and relocate the existing Section 4.2.22 to Section 4.2.22.1.

4.2.22 Coexistence of SISO, MIMO, and Channel Bonding: System Capability Aspect

A single transmitter can be provisioned with multiple capabilities, including SISO, MIMO, and channel bonding operations, as provided by [3] and [5]. Networks utilizing such transmitters may operate extensional technologies like MIMO and channel bonding while enabling individual SISO operations. This means that a single transmitted emission, more specifically a complete delivered product, can include MIMO or channel-bonded PLP(s) along with SISO PLP(s). Alternatively, a single complete delivered product can also consist of MIMO and channel-bonded PLPs while having no SISO PLPs.

This aspect calls for provisions to ensure that receivers with partial capabilities can still access a subset of the complete delivered product. For example, the allocation of LLS accounts for such compatibility (see Section 5.1.1 for details). In the same context, the signaling parameters for Layered MIMO Type B are designed to maintain backward compatibility with SISO receivers that do not support MIMO operations. The provisions for compatibility account for physical capabilities and related scalability of the system. The following examples are worth noting:

- A MIMO-capable transmitter or receiver can perform all SISO operations, but a SISO-capable transmitter or receiver may not necessarily support MIMO operations.
- A transmitter or receiver supporting joint operations of MIMO and channel bonding will also support individual operations of MIMO and channel bonding (and SISO as well). However, a transmitter or receiver that supports only one of those technologies may not necessarily support the combined operation of MIMO and channel bonding.

MIMO, channel bonding, and their joint operations are extensional technologies that can be added to the SISO capability, which is mandatory for all ATSC 3.0 entities. Conversely, entities supporting an extensional technology can operate any functional subsets necessary for the supported extensional technology. This demonstrates the scalability among SISO and extensional technologies.

PHY Functional Scalability (abbreviated as PHY Scalability) is defined in this context to describe the priority for functional compatibility. PHY Scalability can be described by tiers as presented in Table 4.12. A higher tier number represents higher PHY Scalability, with the following meaning: When a technology is marked as Tier *N*, entities supporting this technology also support all technologies with lower PHY Scalability, from Tier 1 to Tier $N-1$. In other words, systems capable of a certain technology will necessarily be able to operate scaled-down operations with lower PHY Scalability.

Tier 1 at the ground level represents the minimum scalability and requires the highest priority for compatibility. SISO and all mandatory technologies belong to Tier 1. Tier 2, representing the next priority, includes MIMO and channel bonding. In essence, MIMO and channel bonding are considered equal in priority unless a specific preference or constraint is predefined. If national or regional preference exists, a tier can be further divided into sub-tiers. For example, if MIMO is deployed first and channel bonding is introduced later, MIMO might have a higher priority than channel bonding. In this case, the country or service region can assign MIMO and channel bonding to Tier 2-1 and Tier 2-2, respectively. Tier 3 is assigned to the combined operation of MIMO and channel bonding (see Section L.13 and O.13 of [3] for details). Combined operations of extensional technologies require provisions for standalone operations of subset technologies and, therefore, take higher tiers than the individual subsets.

Table 4.1 PHY Functional Scalability Tiers

Tier	Technology
Tier 1 (Highest Priority and Lowest Scalability)	Pure SISO
Tier 2	MIMO, Channel Bonding
Tier 3	Combined Operation of MIMO and Channel Bonding

A receiver's accessibility to a PLP is determined by transmission robustness and PHY Scalability.

~~4.2.22~~ 4.2.22.1 SISO Operation of MIMO-Capable Transmission System

When it is possible to include both SISO and MIMO operation alternately in a single transmitted emission, as provided by A/322 and A/324, it is important to establish the correct signal phasing between the two outputs of a MIMO-capable transmitter and through the following portions of the RF system, including the antenna, during SISO portions of the transmission.

Given the two outputs of a MIMO-capable transmitter, when in SISO operation, either one output (Polarization #2) will be muted, or the two outputs will have identical signals on each. (What follows presumes that the Polarization #2 output is not muted during SISO operation but remains active to enable taking advantage of the power available from the combination of the two high-power outputs.) It is assumed in the ATSC 3.0 MIMO system design described that the two outputs will feed a pair of passive RF systems (e.g., mask filters and transmission lines) that connect to a pair of antenna inputs that, in turn, produce a pair of cross-polarized radiated signals.

To obtain optimum performance from the MIMO transmitting antenna with its pair of inputs, when operated in SISO mode, the emitted signals must be both time-coincident and in-phase with one another. In such an arrangement, the two radiated signals will add to create a stronger signal for SISO reception, while, if they are out of time or phase, they will subtract one from the other, resulting in effectively weaker signals at receiver inputs.

For maximum benefit from the addition of power from the two transmitted signals, they should be offset in phase from one another by 90 degrees. This will produce a signal rotating in polarization with one rotation for each cycle of the carrier frequency. Depending on which part of the antenna leads in phase and which one lags, the result will be either left-hand or right-hand circular or elliptical polarization. Either can work, but which should be used may be specified in regulations by a national or regional communications authority. If the power in both polarizations is equal, circular polarization will result upon radiation; if they are unequal, elliptical polarization will result. Most important with respect to the direction of rotation is that, if receivers have only single inputs (i.e., they are not capable of MIMO), they can use circular-polarized receiving antennas to improve reception, but the transmitting and receiving antennas must be designed for the same direction of polarization rotation.

It is worth noting that, in MIMO signal delivery, because different data is being sent in the two polarizations, there will be no signal coherence between the two polarizations of the transmission, thus no power gain as in the circularly polarized SISO case. But the benefit of the additional transmitter capacity nevertheless is obtained in MIMO operation either through sending the same data in both polarizations but coded independently, or through sending up to twice as much data as would be sent in a SISO signal.

Add Sections 4.2.22.1.1, 4.2.22.1.2, 4.2.22.1.3, 4.2.22.1.4, 4.2.22.1.5, and 4.2.22.1.6 as follows:

4.2.22.1.1 Choice of Option 1 or 2 when Transmitting both MIMO and SISO Subframes

When MIMO and SISO subframes are combined in the same RF transmission there are two options presented in L.11.2 of [3]. The broadcaster may wonder which is the best choice for their system. This section describes the background behind why two options are presented, notes on possible implementation difficulties, and provides guidance to broadcasters on the choice of option.

4.2.22.1.2 Background

The major use case to transmit both MIMO and SISO subframes arises in countries where ATSC 3.0 SISO transmissions already exist; MIMO transmission is to be started while the SISO transmission continues, but sufficient new frequency bands are not available to transmit MIMO on a separate RF channel. Thus, the transmission of SISO and MIMO subframes in the same RF channel allows existing SISO-capable receivers to decode the SISO transmission and newer, more advanced MIMO-capable receivers to decode both the SISO and MIMO transmissions.

However, in some regions the polarization of broadcast transmission is specified by regulation and cannot be freely chosen by the broadcaster. For example, only horizontal polarization is allowed for SISO transmissions.

4.2.22.1.3 Further Explanation of Option 1 and Option 2

In L.11.2 of [3] (Option 1) SISO transmission only occurs on one polarization. This is depicted in Figure 4.9.

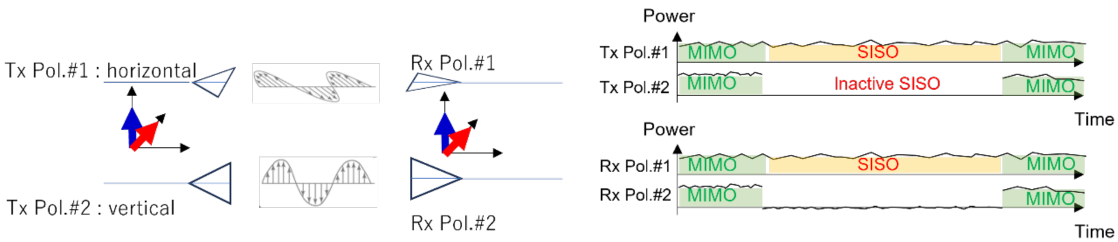

Figure 4.9 Example of Option 1 SISO transmission in MIMO systems.

It will be common (particularly for indoor or mobile reception) for the signal polarization to change due to channel effects such as reflection. In this case, only some of the SISO power in one polarization will be received at the transmitted SISO polarization. This is depicted in Figure 4.10.

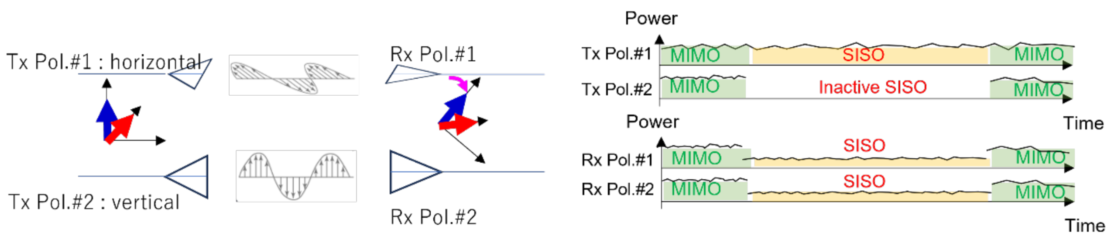

Figure 4.10 Illustration of polarization changes in Option 1 SISO transmission.

4.2.22.1.4 Transmitter Implementation Issues for Option 1

As described above, in the case of Option 1, during the SISO transmission there will times when only one polarization transmission will be active. This must be detected and controlled at the transmitter dynamically, differing from conventional continuous broadcast output.

4.2.22.1.5 Receiver implementation Issues for Option 1

At the receiver there will be a received power difference between the SISO and MIMO signals, which is dependent on the channel effects in each polarization. While the exact effects on the receiver will vary for each receiver design and mitigation measures employed, typically the receiver automatic-gain control circuits will operate to increase the signal level when it is low and decrease again when the SISO transmission begins again. Therefore, it can be expected that there will be performance degradation at the receiver due to imperfections in the channel equalization at the receiver.

4.2.22.1.6 Recommendations for Choice of Option 1 or Option 2

It is recommended that the use of Option 1 or Option 2 be carefully considered and decided on a national level before introduction, with appropriate consideration of the regulatory environment, country requirements and broadcaster needs.

In the absence of any regulatory or commercial requirements, it is recommended to use Option 2, as this provides superior performance and coverage for SISO transmission.

It is recommended that SISO subframes precede MIMO subframes, and that SISO subframes are grouped together followed by a grouping of all MIMO subframes.

Modify Section 5.1.1, "Delivered Product in Multiple PLPs," as follows

5.1.1 Delivered Product in Multiple PLPs

The IP-level signaling information such as Low Level Signaling (LLS), including Service List Table (SLT) and Service Layer Signaling (SLS) [6], and Link Mapping Table (LMT) [4] may be configured in a separate PLP in order to provide different robustness for the signaling information. In such cases, it is strongly recommended that the IP-level signaling information be present in the most robust PLP out of multiple PLPs carrying a complete delivered product. When LDM is used, it is recommended that the IP-level signaling information be present in the most robust Core PLP out of multiple PLPs carrying a complete delivered product.

The carriage of IP-level signaling ensures compatibility with receivers that have the least functional capability in extensional technologies, such as (Layered or non-Layered) MIMO and channel bonding. This aspect is described in terms of PHY Scalability: Receivers with lower PHY Scalability are preferentially supported to maintain maximum compatibility. A complete delivered product may consist of a mixture of SISO PLP(s) and MIMO PLP(s). In such cases, it is strongly recommended that the IP-level signaling information be present in the most robust SISO PLP out of multiple PLPs carrying the complete delivered product. When LDM or Layered MIMO is used in part, it is strongly recommended that the complete delivered product contain the IP-level signaling information in the most robust Core PLP using SISO.

Likewise, when a mixture of channel-bonded PLP(s) and nonbonded PLP(s) assemble a complete delivered product, it is strongly recommended that the complete delivered product contain the IP-level signaling information in the most robust, nonbonded Core PLP out of the engaged PLPs within each RF channel. If nonbonded Core PLP is absent, the IP-level signaling information is included in the most robust Core PLP using channel bonding. Overall, a general rule that accounts for mixed use of SISO, MIMO, Layered MIMO, and channel bonding is as follows: Within each RF channel, it is recommended that the IP-level signaling information be present in the most robust Core PLP that is nonbonded and uses SISO. If no such nonbonded SISO Core PLP exists, the IP-level signaling information should be included in the most robust MIMO Core PLP, applying the one with lower PHY Scalability between MIMO and channel bonding in the service area.

A complete delivered product that may be composed of one or more PLPs should contain the appropriate IP-level signaling information including LLS and LMT. Note that in [4] and [6], the minimum requirement of the LLS and LMT delivery is to be repeated every 5 seconds. For fast service acquisition, it is recommended that the LLS and LMT be sent in every physical layer frame. This would result in setting **L1B_lls_flag** = 1 (for LLS carried in the current frame) and **L1D_plp_lls_flag** = 1 (for LLS carried in the corresponding PLP) in every frame.

Add a new Annex E as follows:

Annex E: Estimation of MIMO System Performance

E.1 INTRODUCTION

This Annex describes a tractable measure to predict the physical layer performance of ATSC 3.0 MIMO systems. The presented is a calculation model that maps SISO system performance onto MIMO system performance, referencing Annex A measurements previously evaluated for ATSC 3.0 SISO systems.

Note: Those C/N values from Annex A already include margins for implementation loss in a SISO reference receiver. For a MIMO reference receiver, an additional implementation loss (e.g., 0.5dB) margin could be added to the C/N values from Annex A.

This estimation model captures the penalty of cross-polarization interference that arises in MIMO channels. The increase in required C/N is identified as dependent on XPD: Given an XPD value as part of the channel condition, the estimation model converts required C/N data in Annex A into performance estimates for the MIMO system using identical ModCod combinations.

E.1.1 System Performance Criteria

System performance in this Annex refers to the minimum C/N required to achieve a QEF condition. The QEF criteria applied to the estimation result are consistent with those used to measure the rationale SISO performance data. The Annex A data were measured at BER = 10^{-6} (i.e., FER = 10^{-4}), and the MIMO C/N estimates deduced therefrom are interpreted to promise the same error performance.

Note that the estimation model may also use other reference datasets (instead of Annex A) measured at different target error rates. The guaranteed error performance should follow the referenced criteria.

The results in this Annex are theoretical estimates relying on optimal MIMO detection (i.e., MIMO equalization) assumption at the receiver. Maximum likelihood (ML) MIMO equalization is assumed for the calculation model, so potential implementation losses can additionally occur when other MIMO detection schemes are used, such as minimum mean-square error (MMSE) methods.

E.1.2 Channel Model Types and Description of XPD

The estimation model is compatible with three types of channel conditions: AWGN, Rayleigh (RL), and Rician (RC). AWGN channel represents a situation where the channel consists solely of line-of-sight (LoS) paths; RL channel depicts the converse where the channel consists solely of non-LoS (NLoS) scatters. RC channel represents the case having both LoS and NLoS components, where the power ratio between those is characterized by Rician *K*-factor.

Formulaic descriptions for the considered channel models are described in Table E.1.1 below,

Table E.1.1 Channel Model Description

Channel Model	Formulaic Description
AWGN (Full-LoS)	$\mathbf{H}_{\mathrm{AWGN}} = \begin{bmatrix} \sqrt{\rho_L} & \sqrt{1-\rho_L} \\ \sqrt{1-\rho_L} & \sqrt{\rho_L} \end{bmatrix}$
RL	$\mathbf{H}_{\mathrm{RL}} = \begin{bmatrix} \sqrt{\rho_N} g_{00} & \sqrt{1-\rho_N} g_{10} \\ \sqrt{1-\rho_N} g_{01} & \sqrt{\rho_N} g_{11} \end{bmatrix}$
RC	$\mathbf{H}_{\mathrm{RC}} = \sqrt{\frac{K}{1+K}} \mathbf{H}_{\mathrm{AWGN}} + \sqrt{\frac{1}{1+K}} \mathbf{H}_{\mathrm{RL}}$

where:

ρ_L denotes a parameter identifying the power portion of co- and cross-polarization components in the LoS part of MIMO channel. This value is determined by $\mathrm{XPD_L}$;

ρ_N denotes a parameter identifying the power portion of co- and cross-polarization components in the NLoS part of MIMO channel. This value is determined by $\mathrm{XPD_N}$;

$\mathrm{XPD_L}$ denotes the XPD evaluated in the LoS part of MIMO channel, described in dB unit;

$\mathrm{XPD_N}$ denotes the XPD evaluated in the NLoS part of MIMO channel, described in dB unit;

g_{00}, g_{10}, g_{01}, g_{11} denote the normalized random fading gain at each MIMO channel entity, which are i.i.d. complex Gaussian random variables with a zero-mean and unit variance;

K is the Rician K-factor, given $K = 10$ in this Annex.

In this Annex, XPD is described in terms of channel XPD incorporating all cross-polarization effects introduced from antennas and propagation paths. XPD in this context denotes the ratio between co- and cross-polarization channel powers. Relationships between ρ_L, ρ_N, $\mathrm{XPD_L}$, and $\mathrm{XPD_N}$ are given as $\mathrm{XPD_L} = 10\log_{10}(\rho_L/(1-\rho_L))$ and $\mathrm{XPD_N} = 10\log_{10}(\rho_N/(1-\rho_N))$, which can be rewritten as:

$$\rho_L = \frac{10^{\frac{\mathrm{XPD_L}}{10}}}{1+10^{\frac{\mathrm{XPD_L}}{10}}} \quad \text{and} \quad \rho_N = \frac{10^{\frac{\mathrm{XPD_N}}{10}}}{1+10^{\frac{\mathrm{XPD_N}}{10}}}, \qquad \text{Eq. (E1)}$$

respectively. Further details on XPD and MIMO channel models are provided in Annex F.

E.1.3 Organization

There is a provision to support erroneous CSI environment in addition to ideal estimation with perfect CSI. The estimation model is categorized into two classes contingent upon the availability of CSI:

- Class P: Perfect CSIR assumed (Section E.2).

- Class E: Channel estimation errors accounted (Section E.3).

Note that the pilot boosting effect is accessible in Class E whereas Class P neglects channel estimation operations.

Both classes are modeled over representative samples of channel conditions. The channel conditions supported are listed in Table E.1.2.

Table E.1.2 Channel XPD Configurations Supported in Estimation Models

Channel Model	**XPD Configuration Θ_{XPD}**	
	XPD in LoS components: $\mathrm{XPD_L}$	**XPD in NLoS components: $\mathrm{XPD_N}$**
AWGN	Any values are applicable if $\mathrm{XPD_L} \geq 0$ dB	N/A (NLoS signals absent)
Rayleigh	N/A (LoS signals absent)	20 dB
		10 dB
		5 dB
		0 dB
Rician	20 dB	20 dB
		10 dB
		5 dB
		0 dB
	10 dB	10 dB
		5 dB
		0 dB

The estimation model presents a unified structure compatible across its subdivided classes and available channel conditions. The general procedure derives τ_{MIMO} from an input variable set $(\tau_{SISO}, ChMod, \Theta_{\mathrm{XPD}})$, where:

τ_{MIMO} denotes the linear scale expression of the required C/N estimate in a MIMO system. The dB scale expression of this C/N value is given by $10\log_{10}\tau_{MIMO}$;

τ_{SISO} denotes the linear scale expression of the reference C/N requirement measured in SISO systems. τ_{SISO} particularly refers to the AWGN channel measurements, i.e., when Annex A is referenced, values in the 'Lab test' or 'Simulation' rows of Table A.3.2 can be used. This value relates to the measurement obtained without applying LDM and pilot boosting. The dB scale expression of this C/N value is given by $10\log_{10}\tau_{SISO}$;

$ChMod$ is a parameter identifying the channel model condition such that $ChMod \in \{\mathrm{AWGN}, \mathrm{RL}, \mathrm{RC}\}$;

Θ_{XPD} is a parameter identifying the channel XPD configuration and is defined as subject to the channel model. If $ChMod = \mathrm{AWGN}$, $\Theta_{\mathrm{XPD}} = \mathrm{XPD_L} \in \{20, 10, 5, 0\}$; if $ChMod = \mathrm{RL}$, $\Theta_{\mathrm{XPD}} = \mathrm{XPD_N} \in \{20, 10, 5, 0\}$; and if $ChMod = \mathrm{RC}$, $\Theta_{\mathrm{XPD}} = (\mathrm{XPD_L}, \mathrm{XPD_N})$ whose available value pairs are specified in Table E.1.2.

When LDM is applied, τ_{MIMO}s for CL and EL are individually obtained (see Section E.2.2 and Section E.3.2). For these cases, the calculation model requires IL as an input variable in addition, where:

IL denotes the injection level described in dB scale. This value is determined by **L1D_plp_ldm_injection_level** and refers to Table 9.24 in [3].

Note that, for LDM examples, only Layered MIMO Type A is supported in the current version of Annex E in this recommended practice.

For Class E model in Section E.3, input variables F_{PB}, D_X, and D_Y are additionally required, where:

F_{PB} denotes the dB scale power of pilot boosting applied to the scattered pilots. This value is determined by **L1D_scattered_pilot_boost** (or **L1B_first_sub_scattered_pilot_boost**) combined with D_X and D_Y, and refers to Table 9.16 in [3];

D_X is the frequency domain separation of pilot bearing carriers, which is determined by **L1D_scattered_pilot_pattern** (or **L1B_first_sub_scattered_pilot_pattern**);

D_Y is the time domain separation of pilot-bearing cells, i.e., the number of symbols forming one scattered pilot sequence, which is determined by **L1D_scattered_pilot_pattern** (or **L1B_first_sub_scattered_pilot_pattern**).

Note: The reference C/N τ_{SISO} uses the values measured in unfaded channels. When Annex A is referenced, values in the 'Lab test' or 'Simulation' rows of Table A.3.2 are recommended. The Annex A values should be converted into linear scale before being used for τ_{SISO} as follows since the Annex A data are recorded in dB scale.

$$\tau_{SISO} = 10^{\frac{\text{Required C/N in SISO System [dB]}}{10}}$$

Conversely, the resultant τ_{MIMO} can be converted into dB scale as follows:

$$\text{dB Scale Estimate of Required C/N in MIMO System [dB]} = 10\log_{10}\tau_{MIMO}$$

E.2 ESTIMATION WITH PERFECT CSI ASSUMPTION (CLASS P MODEL)

This section describes Class P method that assumes perfect CSIR, i.e., no channel estimation error. Class P estimates can be regarded as the theoretical limit that each ModCod combination in ATSC 3.0 MIMO can achieve.

Section E.2.1 presents estimations for non-LDM use cases. Estimations for LDMed systems are provided in Section E.2.2, identifying the CL and EL performances each. Section E.2.3 offers several exercise examples to guide practical applications.

E.2.1 Method Description: Non-LDM Cases

A generalized formula for Class P estimation is outlined as

$$\begin{aligned}\text{Required C/N [dB]} &= 10\log_{10}\tau_{MIMO}\\ &= 10\log_{10}\zeta + f_{co}^{ChMod}(\zeta_{dB} \mid \Theta_{\text{XPD}})\end{aligned} \qquad \text{Eq. (E2)}$$

when LDM is not applied. The linear scale formulation constitutes

$$\tau_{MIMO} = \zeta \times 10^{\frac{f_{co}^{ChMod}(\zeta_{dB} \mid \Theta_{\text{XPD}})}{10}}. \qquad \text{Eq. (E3)}$$

This is composed of an intermediate estimate

$$\zeta = \frac{-1 + \sqrt{1 + \Omega_{ChMod}(\mathcal{E}_R - 1)}}{\Omega_{ChMod}} \qquad \text{Eq. (E4)}$$

and a correction offset function $f_{co}^{ChMod}(\zeta_{dB} \mid \Theta_{\mathrm{XPD}})$, where $\zeta_{dB} = 10\log_{10}\zeta$. Note that each $ChMod$ realization (i.e., AWGN, RL, or RC) has a unique $f_{co}^{ChMod}(\zeta_{dB} \mid \Theta_{\mathrm{XPD}})$. Sections E.2.1.1, E.2.1.2, and E.2.1.3 detail their respective definitions.

The parameters $\mathcal{E}_R$ and Ω_{ChMod} are specified as

$$\mathcal{E}_R = 1 + 2\tau_{SISO} + \tau_{SISO}^2 \qquad \text{Eq. (E5)}$$

and

$$\Omega_{ChMod} = \begin{cases} \Omega_{\mathrm{AWGN}} & ChMod = \mathrm{AWGN} \\ \Omega_{\mathrm{RL}} & ChMod = \mathrm{RL} \\ \Omega_{\mathrm{RC}} & ChMod = \mathrm{RC} \end{cases}, \qquad \text{Eq. (E6)}$$

given as dependent on τ_{SISO} and $ChMod$, respectively. Each realization of Ω_{ChMod} is a scalar coefficient solely determined by XPD values; and is quantified in Sections E.2.1.1, E.2.1.2, and E.2.1.3.

The estimation procedure computing τ_{MIMO} unfolds as follows:

Input:	τ_{SISO}, $ChMod$, Θ_{XPD}
Initialization:	Compute $\mathcal{E}_R$ and Ω_{ChMod}.
Step i:	Compute ζ using Eq. (E4).
Step ii:	Obtain τ_{MIMO} by applying $f_{co}^{ChMod}(\zeta_{dB} \mid \Theta_{\mathrm{XPD}})$, using $\zeta_{dB} = 10\log_{10}\zeta$.
Output:	τ_{MIMO}

E.2.1.1 AWGN Channel (Full-LoS)

Only LoS components are present in AWGN channels, so the effective XPD in AWGN channels directly equals $\mathrm{XPD_L}$. $\mathrm{XPD_N}$ is not defined for this type of channel, and hence the following holds: $\Theta_{\mathrm{XPD}} = \mathrm{XPD_L}$.

Given ρ_L by Eq. (E1), the parameter Ω_{ChMod} is specified as

$$\Omega_{\mathrm{AWGN}} = (2\rho_L - 1)^2. \qquad \text{Eq. (E7)}$$

For every instance of AWGN channel, $f_{co}^{ChMod}(\zeta_{dB} \mid \Theta_{\mathrm{XPD}}) = 0$ holds regardless of any ζ_{dB} and Θ_{XPD}. Simply,

$$\tau_{MIMO} = \begin{cases} \dfrac{-1 + \sqrt{1 + (2\rho_L - 1)^2(2\tau_{SISO} + \tau_{SISO}^2)}}{(2\rho_L - 1)^2} & \rho_L > \dfrac{1}{2}\ (\mathrm{XPD_L} > 0) \\ \tau_{SISO} + \dfrac{\tau_{SISO}^2}{2} & \rho_L = \dfrac{1}{2}\ (\mathrm{XPD_L} = 0) \end{cases}$$

holds in AWGN channel.

Note that this calculation model under AWGN channel condition allows any real-valued ρ_L within a range of $\frac{1}{2} < \rho_L \leq 1$. This means that any $\mathrm{XPD_L} \geq 0$ are supported when AWGN environment is considered.

E.2.1.2 Rayleigh Channel

Conversely to AWGN channels, only NLoS components are present in RL channels. The effective XPD in RL channels directly equals $\mathrm{XPD_N}$. $\mathrm{XPD_L}$ is not defined for this type of channel, and hence the following holds: $\Theta_{\mathrm{XPD}} = \mathrm{XPD_N}$.

Given ρ_N by Eq. (E1), the parameter Ω_{ChMod} is specified as

$$\Omega_{\mathrm{RL}} = {\rho_N}^2 + (1-\rho_N)^2. \qquad \text{Eq. (E8)}$$

When conditioned on RL channel, a correction offset function

$$f_{co}^{\mathrm{RL}}(\zeta_{dB} \mid \Theta_{\mathrm{XPD}}) = \begin{cases} c_5\zeta_{dB}^5 + c_4\zeta_{dB}^4 + c_3\zeta_{dB}^3 + c_2\zeta_{dB}^2 + c_1\zeta_{dB} + c_0 & \zeta_{dB} < 30 \\ f_{sat}^{\mathrm{RL}} & \zeta_{dB} \geq 30 \end{cases} \qquad \text{Eq. (E9)}$$

applies to Eq. (E3) (see **Step ii** of the estimation procedure described in Section E.2.1). The coefficients c_5, c_4, …, c_0 constructing $f_{co}^{\mathrm{RL}}(\zeta_{dB} \mid \Theta_{\mathrm{XPD}})$ refer to Table E.2.1 below. Note that these coefficient values are also specific to $\mathrm{XPD_N}$.

Table E.2.1 Coefficients of $f_{co}^{\mathrm{RL}}(\zeta_{dB} \mid \Theta_{\mathrm{XPD}})$ w.r.t. XPD Levels

XPD Configuration: $\mathrm{XPD_N}$	Coefficients					
	c_5	c_4	c_3	c_2	c_1	c_0
20 dB	-1.237×10^{-7}	1.156×10^{-5}	-3.366×10^{-4}	8.187×10^{-4}	0.117	0.9813
10 dB	-1.263×10^{-7}	1.225×10^{-5}	-3.841×10^{-4}	2×10^{-3}	0.108	0.8518
5 dB	-9.448×10^{-8}	1.005×10^{-5}	-3.544×10^{-4}	2.814×10^{-3}	8.911×10^{-2}	0.6548
0 dB	-5.598×10^{-8}	7.061×10^{-6}	-2.891×10^{-4}	2.997×10^{-3}	6.902×10^{-2}	0.4957

Eq. (E9) relates that $f_{co}^{\mathrm{RL}}(\zeta_{dB} \mid \Theta_{\mathrm{XPD}})$ is saturated by f_{sat}^{RL} when $\zeta_{dB} \geq 30$ dB. Table E.2.2 specifies this value f_{sat}^{RL} according to $\mathrm{XPD_N}$.

Table E.2.2 Values of f_{sat}^{RL} w.r.t. XPD Levels

XPD Configuration: $\mathrm{XPD_N}$	f_{sat}^{RL} [dB]
20 dB	2.5
10 dB	2.42
5 dB	2.14
0 dB	1.83

E.2.1.3 Rician Channel

RC channel represents a compound of AWGN and RL channel responses where both LoS and NLoS components are present. $\mathrm{XPD_L}$ and $\mathrm{XPD_N}$ are individually realized in RC channels, so the XPD condition $\Theta_{\mathrm{XPD}} = (\mathrm{XPD_L}, \mathrm{XPD_N})$ is defined as a pair consisting of $\mathrm{XPD_L}$ and $\mathrm{XPD_N}$. The effective XPD can be derived therefrom as described in Annex F.

Given ρ_L and ρ_N by Eq. (E1), the parameter Ω_{ChMod} is specified as

$$\Omega_{\mathrm{RC}} = \left(\frac{\rho_L K}{1+K} + \frac{\rho_N}{1+K}\right)^2 + \left(\frac{(1-\rho_L)K}{1+K} + \frac{(1-\rho_N)}{1+K}\right)^2 - \frac{2\rho_L(1-\rho_L)K^2}{(1+K)^2}. \qquad \text{Eq. (E10)}$$

Note here that the Rician K-factor is given as $K = 10$ throughout this Annex.

When conditioned on RC channel, a correction offset function

$$f_{co}^{\mathrm{RC}}(\zeta_{dB} \mid \Theta_{\mathrm{XPD}}) = \begin{cases} c_5\zeta_{dB}^5 + c_4\zeta_{dB}^4 + c_3\zeta_{dB}^3 + c_2\zeta_{dB}^2 + c_1\zeta_{dB} + c_0 & \zeta_{dB} < 30 \\ f_{sat}^{\mathrm{RC}} & \zeta_{dB} \geq 30 \end{cases} \quad \text{Eq. (E11)}$$

applies to Eq. (E3) (see **Step ii** of the estimation procedure described in Section E.2.1). The coefficients $c_5, c_4, \ldots, c_0$ constructing $f_{co}^{\mathrm{RC}}(\zeta_{dB} \mid \Theta_{\mathrm{XPD}})$ refer to Table E.2.3 below. Note that these coefficient values are also specific to the pair ($\mathrm{XPD_L}$, $\mathrm{XPD_N}$).

Table E.2.3 Coefficients of $f_{co}^{\mathrm{RC}}(\zeta_{dB} \mid \Theta_{XPD})$ w.r.t. XPD Levels

XPD Configuration		Coefficients					
$\mathrm{XPD_L}$	$\mathrm{XPD_N}$	c_5	c_4	c_3	c_2	c_1	c_0
20 dB	20 dB	-2.504×10^{-8}	2.234×10^{-6}	-5.701×10^{-5}	-1.261×10^{-4}	2.266×10^{-2}	0.1916
	10 dB	-1.961×10^{-8}	1.782×10^{-6}	-4.566×10^{-5}	-1.64×10^{-4}	2.088×10^{-2}	0.1766
	5 dB	-1.784×10^{-8}	1.625×10^{-6}	-4.239×10^{-5}	-9.539×10^{-5}	1.764×10^{-2}	0.1478
	0 dB	-1.073×10^{-8}	9.887×10^{-7}	-2.627×10^{-5}	-6.453×10^{-5}	1.193×10^{-2}	9.908×10^{-2}
10 dB	10 dB	-3.442×10^{-8}	3.416×10^{-6}	-1.072×10^{-4}	5.958×10^{-4}	2.508×10^{-2}	0.1751
	5 dB	-2.896×10^{-8}	2.944×10^{-6}	-9.511×10^{-5}	5.922×10^{-4}	2.127×10^{-2}	0.1466
	0 dB	-1.965×10^{-8}	2.109×10^{-6}	-7.294×10^{-5}	5.714×10^{-4}	1.458×10^{-2}	9.731×10^{-2}

Note also that $f_{co}^{\mathrm{RC}}(\zeta_{dB} \mid \Theta_{\mathrm{XPD}})$ is saturated by f_{sat}^{RC} when $\zeta_{dB} \geq 30$ dB. Table E.2.4 specifies this value f_{sat}^{RC} according to ($\mathrm{XPD_L}$, $\mathrm{XPD_N}$).

Table E.2.4 Values of f_{sat}^{RC} and Thresholds of Saturation w.r.t. XPD Levels

XPD Configuration		f_{sat}^{RC} [dB]
$\mathrm{XPD_L}$	$\mathrm{XPD_N}$	
20 dB	20 dB	0.42
	10 dB	0.39
	5 dB	0.33
	0 dB	0.23
10 dB	10 dB	0.5
	5 dB	0.43
	0 dB	0.31

E.2.2 Estimations in LDM Scenarios (Layered MIMO Type A)

This section illustrates Class P estimations for LDM systems. Note that every LDM example in this Annex refers to Layered MIMO, the combined use of LDM and MIMO (see Annex O in [3]). The presented model specifically applies to Layered MIMO Type A, in which both the CL and EL use MIMO. τ_{MIMO} is accordingly identified for each LDM layer in the following subsections.

E.2.2.1 Core Layer

For explicit identification, the τ_{MIMO} of CL in LDM signals is designated by $\tau_{MIMO}|_{LDM\ CL}$. A Class P estimation model yields a formula

$$\tau_{MIMO}|_{LDM\ CL} = \frac{\hat{\zeta}_{CL}}{1-\Delta_{LDM}-\Delta_{LDM}\hat{\zeta}_{CL}} \qquad \text{Eq. (E12)}$$

where a latent variable $\hat{\zeta}_{CL}$ is given as

$$\hat{\zeta}_{CL} = \zeta_{CL} \times 10^{\frac{f_{co}^{ChMod}(\zeta_{CL}^{dB}\,|\,\Theta_{\mathrm{XPD}})}{10}} \qquad \text{Eq. (E13)}$$

for another latent variable ζ_{CL} and $f_{co}^{ChMod}\left(\zeta_{CL}^{dB}\,|\,\Theta_{\mathrm{XPD}}\right)$. Note that the same $f_{co}^{ChMod}(\cdot)$ as in Section E.2.1 shall be used while holding $\zeta_{CL}^{dB} = 10\log_{10}\zeta_{CL}$ as input.

$$\zeta_{CL} = \frac{(1-\Delta_{LDM})\zeta}{1+\Delta_{LDM}\zeta} \qquad \text{Eq. (E14)}$$

The parameters and ζ and Δ_{LDM} determining ζ_{CL} are given by

$$\zeta = \frac{\mathcal{E}_R\Delta_{LDM} - 1 + \sqrt{(\mathcal{E}_R\Delta_{LDM}-1)^2 + \Omega_{ChMod}(1-\mathcal{E}_R\Delta_{LDM}^2)(\mathcal{E}_R - 1)}}{\Omega_{ChMod}(1-\mathcal{E}_R\Delta_{LDM}^2)} \qquad \text{Eq. (E15)}$$

and

$$\Delta_{LDM} = \frac{10^{-\frac{IL}{10}}}{1+10^{-\frac{IL}{10}}}, \qquad \text{Eq. (E16)}$$

respectively. $\mathcal{E}_R$ and Ω_{ChMod} herein share the definitions in Section E.2.1.

The estimation procedure computing τ_{MIMO} unfolds as follows:

Input:	τ_{SISO}, $ChMod$, Θ_{XPD}, IL
Initialization:	Compute $\mathcal{E}_R$, Ω_{ChMod}, and Δ_{LDM}. See Eqs. (E5), (E6), and (E16).
Step i:	Compute ζ using Eq. (E15).
Step ii:	Convert ζ into ζ_{CL} using Eq. (E14).
Step iii:	Obtain $\hat{\zeta}_{CL}$ by applying $f_{co}^{ChMod}\left(\zeta_{CL}^{dB}\,|\,\Theta_{\mathrm{XPD}}\right)$, using $\zeta_{CL}^{dB} = 10\log_{10}\zeta_{CL}$ and Eq. (E13).
Step iv:	Obtain $\tau_{MIMO}|_{LDM\ CL}$ from Eq. (E12).
Output:	$\tau_{MIMO}|_{LDM\ CL}$

Note above that $\tau_{MIMO}|_{LDM\ CL}$ directly agree with ζ (i.e., $\tau_{MIMO}|_{LDM\ CL} = \zeta$) when $ChMod$ = AWGN.

Note: The τ_{SISO} value corresponds to the measurement obtained without applying LDM.

E.2.2.2 Enhanced Layer

When the τ_{MIMO} of LDM EL is denoted as $\tau_{MIMO}|_{LDM\ EL}$, Class P finds the corresponding equation as

$$\tau_{MIMO|LDM\ EL} = \frac{\zeta}{\Delta_{LDM}} \times 10^{\frac{f_{co}^{ChMod}(\zeta_{dB}\,|\,\Theta_{\mathrm{XPD}})}{10}}$$
$$= \frac{-1+\sqrt{1+\Omega_{ChMod}(\mathcal{E}_R-1)}}{\Omega_{ChMod}\Delta_{LDM}} \times 10^{\frac{f_{co}^{ChMod}(\zeta_{dB}\,|\,\Theta_{\mathrm{XPD}})}{10}}, \qquad \text{Eq. (E17)}$$

where the related parameters are given by

$$\zeta = \frac{-1+\sqrt{1+\Omega_{ChMod}(\mathcal{E}_R-1)}}{\Omega_{ChMod}},$$

$\Delta_{LDM} = 10^{-\frac{IL}{10}} / \left(1+10^{-\frac{IL}{10}}\right)$, and by Eq. (E5). The same Ω_{ChMod} and $f_{co}^{ChMod}(\cdot)$ as in Section E.2.1 shall be applied also.

The estimation proceeds with the same as which described in Section E.2.1 but divides the result by Δ_{LDM} in addition. This procedure corresponds with the following.

Input:	τ_{SISO}, $ChMod$, Θ_{XPD}, IL
Initialization:	Compute $\mathcal{E}_R$, Ω_{ChMod}, and Δ_{LDM}. See Eqs. (E5), (E6), and (E16).
Step i:	Compute ζ using Eq. (E4).
Step ii:	Obtain $\tau_{MIMO}|_{LDM\ EL}$ by applying $f_{co}^{ChMod}(\zeta_{dB}|\Theta_{\mathrm{XPD}})$ to ζ/Δ_{LDM}. See Eq. (E17).
Output:	$\tau_{MIMO}|_{LDM\ EL}$

Note: The τ_{SISO} value corresponds to the measurement obtained without applying LDM.

E.2.3 Calculation Examples

Example calculations are given below assuming:

τ_{SISO} 1.9588 (= 2.92 dB)

$ChMod$ RL

Θ_{XPD} $\mathrm{XPD_N}$ = 10 dB ($\mathrm{XPD_L}$ = N/A)

Note: The considered value of τ_{SISO} refers to a ModCod combination described in Table E.2.5. The simulation result in Table A.3.2 is used. Note that the target QEF condition inherits BER = 10^{-6} (used in Table A.3.2) thereby.

Table E.2.5 ModCod Combination for Calculation Examples

Constellation	**16QAM**
Inner Code	LDPC Code (Code Length: 64,800 bits, Code Rate: 5/15)
Outer Code	BCH Code

Based on input parameters above, the initialization step prepares parameters computed as:

$\mathcal{E}_R \quad = 1 + 2 \times 1.9588 + (1.9588)^2 = 8.7548$

$\rho_N \quad = 10^{\frac{10}{10}}/(1 + 10^{\frac{10}{10}}) = 0.9091$

$\Omega_{\mathrm{RL}} \quad = (0.9091)^2 + (1 - 0.9091)^2 = 0.8347$

These parameter values are uniformly applied to both non-LDM and LDM examples that follow.

E.2.3.1 Non-LDM Example

Based on the parameter set described above, Class P estimation for non-LDM configuration proceeds as follows.

ζ and ζ_{dB} are computed as:

$$\zeta = \frac{\left(-1 + \sqrt{1 + 0.8347 \times (8.7548 - 1)}\right)}{0.8347} = 2.0770$$

$$\zeta_{dB} = 10\log_{10} 2.0770 = 3.1743$$

$f_{co}^{\mathrm{RL}}(\zeta_{dB} \mid \Theta_{XPD})$ is computed as:

$$\begin{aligned} f_{co}^{\mathrm{RL}}(3.1743 \mid \mathrm{XPD_N} = 10\ \mathrm{dB}) &= -1.263 \times 10^{-7} \times (3.1743)^5 + 1.225 \times 10^{-5} \times (3.1743)^4 \\ &\quad - 3.841 \times 10^{-4} \times (3.1743)^3 + 2 \times 10^{-3} \times (3.1743)^2 + 0.108 \times \\ &\quad (3.1743) + 0.8518 \\ &= 1.2037 \end{aligned}$$

The estimate τ_{MIMO} is then derived as

$$\tau_{MIMO} = 2.0770 \times 10^{\frac{1.2037}{10}} = 2.7403$$

and leads to the dB scale estimate

$$10\log_{10}\tau_{MIMO} \qquad 4.3780\ \mathrm{dB}.$$

E.2.3.2 LDM Example

LDM examples are given below assuming:

IL 10 dB

The initialization step additionally prepares a parameter computed therefrom:

$$\Delta_{LDM} = 10^{-\frac{10}{10}}/(1 + 10^{-\frac{10}{10}}) = 0.0909$$

This LDM parameter value is uniformly applied to both CL and EL examples that follow.

E.2.3.2.1 Core Layer Example

ζ for CL is computed as:

$$\zeta = \frac{\left(8.7548\times0.0909-1+\sqrt{(8.7548\times0.0909-1)^2+0.8347\times(1-8.7548\times0.0909^2)\times(8.7548-1)}\right)}{0.8347\times(1-8.7548\times0.0909^2)} = 2.9120$$

ζ_{CL} and ζ_{CL}^{dB} are computed as:

$$\zeta_{CL} = \frac{(1-0.0909)\times 2.9120}{1+0.0909\times 2.9120} = 2.0932$$

$$\zeta_{CL}^{dB} = 10\log_{10} 2.0932 = 3.2080$$

$f_{co}^{\mathrm{RL}}\left(\zeta_{CL}^{dB} \mid \Theta_{XPD}\right)$ is computed as:

$$\begin{aligned} f_{co}^{\mathrm{RL}}(3.2080 \mid \mathrm{XPD_N} = 10\ \mathrm{dB}) &= -1.263\times10^{-7}\times(3.2080)^5 + 1.225\times10^{-5}\times(3.2080)^4 \\ &\quad - 3.841\times10^{-4}\times(3.2080)^3 + 2\times10^{-3}\times(3.2080)^2 + 0.108\times \\ &\quad (3.2080) + 0.8518 \\ &= 1.2074 \end{aligned}$$

$\hat{\zeta}_{CL}$ is computed as:

$$\hat{\zeta}_{CL} = 2.0932\times 10^{\frac{1.2074}{10}} = 2.7641$$

The estimate $\tau_{MIMO}|_{LDM\ CL}$ is then derived as

$$\tau_{MIMO}|_{LDM\ CL} = \frac{2.7641}{1-0.0909-0.0909\times 2.7641} = 4.2019$$

and leads to the dB scale estimate

$$10\log_{10}\tau_{MIMO}|_{LDM\ CL} \qquad 6.2344\ \mathrm{dB}.$$

E.2.3.2.2 Enhanced Layer Example

ζ and ζ_{dB} for EL is computed as:

$$\zeta = \frac{\left(-1+\sqrt{1+0.8347\times(8.7548-1)}\right)}{0.8347} = 2.0770$$

$$\zeta_{dB} = 10\log_{10} 2.0770 = 3.1743$$

$f_{co}^{\mathrm{RL}}(\zeta_{dB} \mid \Theta_{XPD})$ is computed as:

$$\begin{aligned} f_{co}^{\mathrm{RL}}(3.1744 \mid \mathrm{XPD_N} = 10\ \mathrm{dB}) &= -1.263\times10^{-7}\times(3.1744)^5 + 1.225\times10^{-5}\times(3.1744)^4 \\ &\quad - 3.841\times10^{-4}\times(3.1744)^3 + 2\times10^{-3}\times(3.1744)^2 + 0.108\times \\ &\quad (3.1744) + 0.8518 \\ &= 1.2037 \end{aligned}$$

The estimate $\tau_{MIMO}|_{LDM\ EL}$ is then derived as

$$\tau_{MIMO}|_{LDM\ EL} = \frac{2.0770}{0.0909} \times 10^{\frac{1.2037}{10}} = 30.147$$

and leads to the dB scale estimate

$$10 \log_{10} \tau_{MIMO}|_{LDM\ CL} \qquad 14.792 \text{ dB.}$$

E.3 ESTIMATION WITH CHANNEL ESTIMATION ERRORS (CLASS E MODEL)

Class E method accounts for erroneous CSIR. The figure of CSI errors is modeled through an actual channel estimation process, provisioning a comprehensive scaling according to the impact of pilot boosting on system performance. Note that Class E method assumes a theoretical channel estimation operation, namely, linear MMSE estimation. The system performance of commercial receivers may vary depending on the channel estimation schemes they implement.

Basic approaches for non-LDM configurations are presented in Section E.3.1 subject to different channel conditions. Estimations under Layered MIMO configurations (specifically Type A) are provided in Section E.3.2. Section E.3.3 offers several exercise examples to guide practices.

Note: The referenced τ_{SISO} values relate to the measurements obtained without applying LDM and pilot boosting.

E.3.1 Non-LDM Case

E.3.1.1 AWGN Channel (Full-LoS)

When conditioned on AWGN channel, channel estimation errors are neglected. Class E estimation in this case corresponds to Class P estimation described in Section E.2.2.1 unless pilot boosting is applied.

When pilot boosting effect applies, the result amounts to $\tau_{MIMO} = \zeta/\kappa_d$ where ζ and κ_d refer to Eq. (E4) and

$$\kappa_d = \frac{1}{1 - \frac{1}{D_X D_Y} + \frac{A_{SP}^2}{D_X D_Y}}, \qquad \text{Eq. (E18)}$$

respectively. This κ_d above quantifies the power reduction at the data cells that offsets boosted pilots. Following the notation in Section 8 of [3], A_{SP} denotes the amplitude in scattered pilot cells and is given by

$$A_{SP} = 10^{\frac{F_{PB}}{20}} \qquad \text{Eq. (E19)}$$

reliant on the pilot boosting power F_{PB}. F_{PB} refers to Table 9.16 in [3] and is determined by **L1D_scattered_pilot_boost** (or **L1B_first_sub_scattered_pilot_boost**) in conjunction with the scattered pilot pattern (D_X and D_Y). Note that A_{SP} is interpreted as an amplitude gain in the context of pilot boosting since Table 9.17 is described to normalize the non-boosted pilot power as 1.

E.3.1.2 Rayleigh Channel

As described in Section E.2.1.2, only NLoS components are present in RL channels. $\Theta_{\mathrm{XPD}} = \mathrm{XPD_N}$ and $\Omega_{\mathrm{RL}} = {\rho_N}^2 + (1-\rho_N)^2$ hold, where Eq. (E1) gives ρ_N.

When conditioned on RL channel (i.e., $ChMod$ = RL), τ_{MIMO} amounts to

$$\tau_{MIMO} = \frac{(A_{SP}^2 + \kappa_d)\hat{\zeta} + \sqrt{\left((A_{SP}^2 + \kappa_d)\hat{\zeta}\right)^2 + 4A_{SP}^2\kappa_d\hat{\zeta}}}{2A_{SP}^2\kappa_d} \qquad \text{Eq. (E20)}$$

whereby A_{SP} and κ_d refer to Eq. (E19) and Eq. (E18) shown in Section E.3.1.1, and where

$$\hat{\zeta} = \zeta \times 10^{\frac{f_{co}^{\mathrm{RL|CE}}(\zeta_{dB} \mid \Theta_{XPD})}{10}}. \qquad \text{Eq. (E21)}$$

If pilot boosting is not applied, Eq. (E20) can be further simplified into $\tau_{MIMO} = \hat{\zeta} + \sqrt{\hat{\zeta}^2 + \hat{\zeta}}$. The intermediate estimate $\hat{\zeta}$ consists of another intermediate estimate

$$\zeta = \frac{-1 + \sqrt{1 + \Omega_{\mathrm{RL}}(\mathcal{E}_R - 1)}}{\Omega_{\mathrm{RL}}} \qquad \text{Eq. (E22)}$$

and a correction offset function

$$f_{co}^{\mathrm{RL|CE}}(\zeta_{dB} \mid \Theta_{\mathrm{XPD}}) = \begin{cases} c_5\zeta_{dB}^5 + c_4\zeta_{dB}^4 + c_3\zeta_{dB}^3 + c_2\zeta_{dB}^2 + c_1\zeta_{dB} + c_0 & \zeta_{dB} < 30 \\ f_{sat}^{\mathrm{RL|CE}} & \zeta_{dB} \geq 30 \end{cases}, \qquad \text{Eq. (E23)}$$

where $\mathcal{E}_R$ is determined from τ_{SISO} by Eq. (E5), and $\zeta_{dB} = 10\log_{10}\zeta$.

Note that this $f_{co}^{\mathrm{RL|CE}}(\cdot)$ differs from the $f_{co}^{\mathrm{RL}}(\cdot)$ shown in Section E.2.1.2. The coefficients c_5, c_4, …, c_0 constituting $f_{co}^{\mathrm{RL|CE}}(\zeta_{dB} \mid \Theta_{\mathrm{XPD}})$ refer to Table E.3.1 below.

Table E.3.1 Coefficients of $f_{co}^{\mathrm{RL|CE}}(\zeta_{dB} \mid \Theta_{\mathrm{XPD}})$ w.r.t. XPD Levels

XPD Configuration: $\mathrm{XPD_N}$	**Coefficients**					
	c_5	c_4	c_3	c_2	c_1	c_0
20 dB	-1.761×10^{-7}	1.571×10^{-5}	-4.391×10^{-4}	1.377×10^{-3}	0.1255	0.9056
10 dB	-1.6×10^{-7}	1.485×10^{-5}	-4.469×10^{-4}	2.345×10^{-3}	0.1149	0.7823
5 dB	-1.072×10^{-7}	1.141×10^{-5}	-4.008×10^{-4}	3.255×10^{-3}	9.319×10^{-2}	0.5874
0 dB	-6.628×10^{-8}	8.22×10^{-6}	-3.313×10^{-4}	3.483×10^{-3}	7.17×10^{-2}	0.4319

Note in Eq. (E23) also that $f_{co}^{\mathrm{RL|CE}}(\zeta_{dB} \mid \Theta_{\mathrm{XPD}})$ is saturated by $f_{sat}^{\mathrm{RL|CE}}$ when $\zeta_{dB} \geq 30$ dB. Table E.3.2 specifies this value $f_{sat}^{\mathrm{RL|CE}}$ according to $\mathrm{XPD_N}$.

Table E.3.2 Values of $f_{sat}^{\mathrm{RL|CE}}$ w.r.t. XPD Levels

XPD Configuration: $\mathrm{XPD_N}$	$f_{sat}^{\mathrm{RL|CE}}$ **[dB]**
20 dB	2.5

10 dB	2.41
5 dB	2.14
0 dB	1.83

Briefly, Class E method involves one more step extracting Eq. (E20) from Eq. (E21) compared to Class P process. A stepwise description of the estimation procedure is as follows:

Input: τ_{SISO}, $ChMod$ = RL, Θ_{XPD}, F_{PB}, D_{X}, D_{Y}

Initialization: Compute $\mathcal{E}_R$, Ω_{RL}, A_{SP}, κ_d. See Eqs. (E5), (E8), (E19), and (E18).

Step i: Compute ζ using Eq. (E22).

Step ii: Obtain $\hat{\zeta}$ by applying $f_{co}^{\mathrm{RL|CE}}(\zeta_{dB} \mid \Theta_{\mathrm{XPD}})$, using $\zeta_{dB} = 10\log_{10}\zeta_{CL}$ and Eq. (E21).

Step iii: Convert $\hat{\zeta}$ into τ_{MIMO} using Eq. (E20).

Output: τ_{MIMO}

E.3.1.3 Rician Channel

As described in Section E.2.1.3, LoS and NLoS components are both present in RC channels. $\mathrm{XPD_L}$ and $\mathrm{XPD_N}$ are individually defined, and the pair of them constitutes $\Theta_{\mathrm{XPD}} = (\mathrm{XPD_L}, \mathrm{XPD_N})$. For RC examples, Ω_{RC} is given by Eq. (E10) where ρ_L and ρ_N refer to Eq. (E1).
When conditioned on RC channel (i.e., $ChMod$ = RC), τ_{MIMO} amounts to

$$\tau_{MIMO} = \frac{(A_{SP}^2+\kappa_d)\hat{\zeta} - (1+K)\kappa_d + \sqrt{\left((A_{SP}^2+\kappa_d)\hat{\zeta} - (1+K)\kappa_d\right)^2 + 4A_{SP}^2\kappa_d(1+K)\hat{\zeta}}}{2A_{SP}^2\kappa_d} \quad \text{Eq. (E24)}$$

whereby A_{SP} and κ_d refer to Eq. (E19) and Eq. (E18) shown in Section E.3.1.1, and where

$$\hat{\zeta} = \zeta \times 10^{\frac{f_{co}^{\mathrm{RC|CE}}(\zeta_{dB} \mid \Theta_{\mathrm{XPD}})}{10}}. \quad \text{Eq. (E25)}$$

This intermediate estimate $\hat{\zeta}$ consists of another intermediate estimate

$$\zeta = \frac{-1+\sqrt{1+\Omega_{\mathrm{RC}}(\mathcal{E}_R - 1)}}{\Omega_{\mathrm{RC}}} \quad \text{Eq. (E26)}$$

and a correction offset function

$$f_{co}^{\mathrm{RC|CE}}(\zeta_{dB} \mid \Theta_{\mathrm{XPD}}) = \begin{cases} c_5\zeta_{dB}^5 + c_4\zeta_{dB}^4 + c_3\zeta_{dB}^3 + c_2\zeta_{dB}^2 + c_1\zeta_{dB} + c_0 & \zeta_{dB} < Th(\Theta_{\mathrm{XPD}}) \\ f_{sat}^{\mathrm{RC|CE}} & \zeta_{dB} \geq Th(\Theta_{\mathrm{XPD}}) \end{cases} \quad \text{Eq. (E27)}$$

where $\mathcal{E}_R$ is determined from τ_{SISO} by Eq. (E5), and $\zeta_{dB} = 10\log_{10}\zeta$.

Note that this $f_{co}^{\mathrm{RC|CE}}(\cdot)$ differs from the $f_{co}^{\mathrm{RC}}(\cdot)$ shown in Section E.2.1.3. The coefficients c_5, c_4, …, c_0 constituting $f_{co}^{\mathrm{RC|CE}}(\zeta_{dB} \mid \Theta_{\mathrm{XPD}})$ refer to Table E.3.3 below. The coefficient values are also specific to ($\mathrm{XPD_L}$, $\mathrm{XPD_N}$).

Table E.3.3 Coefficients of $f_{co}^{\mathrm{RC|CE}}(\zeta_{dB} \mid \Theta_{\mathrm{XPD}})$ w.r.t. XPD Levels

XPD Configuration		Coefficients					
$\mathrm{XPD_L}$	$\mathrm{XPD_N}$	c_5	c_4	c_3	c_2	c_1	c_0
20 dB	20 dB	0	0	0	-5.331×10^{-6}	3.715×10^{-4}	0.416
	10 dB	0	0	-1.296×10^{-6}	8.327×10^{-5}	-1.628×10^{-3}	0.3982
	5 dB	0	0	-3.408×10^{-6}	2.372×10^{-4}	-5.249×10^{-3}	0.3658
	0 dB	3.05×10^{-8}	-2.178×10^{-6}	4.31×10^{-5}	1.382×10^{-4}	-1.185×10^{-2}	0.3149
10 dB	10 dB	0	7.126×10^{-8}	-2.277×10^{-6}	-1.175×10^{-4}	5.261×10^{-3}	0.4544
	5 dB	0	0	0	-1.566×10^{-5}	1.07×10^{-3}	0.4214
	0 dB	2.311×10^{-8}	-1.652×10^{-6}	3.44×10^{-5}	5.056×10^{-6}	-6.783×10^{-3}	0.367

Note in Eq. (E27) also that $f_{co}^{\mathrm{RC|CE}}(\zeta_{dB} \mid \Theta_{\mathrm{XPD}})$ is saturated by $f_{sat}^{\mathrm{RC|CE}}$ when $\zeta_{dB} \geq Th(\Theta_{\mathrm{XPD}})$. The values of $f_{sat}^{\mathrm{RC|CE}}$ and $Th(\Theta_{\mathrm{XPD}})$ according to Θ_{XPD} are specified in Table E.3.4.

Table E.3.4 Values of $f_{sat}^{\mathrm{RC|CE}}$ and Thresholds of Saturation w.r.t. XPD Levels

XPD Configuration		$f_{sat}^{\mathrm{RC|CE}}$ [dB]	$Th(\Theta_{\mathrm{XPD}})$ [dB]
$\mathrm{XPD_L}$	$\mathrm{XPD_N}$		
20 dB	20 dB	0.42	25
	10 dB	0.39	20
	5 dB	0.33	20
	0 dB	0.22	20
10 dB	10 dB	0.5	20
	5 dB	0.44	30
	0 dB	0.32	20

A stepwise description of the estimation procedure is as follows:

Input:	τ_{SISO}, $ChMod$ = RC, K = 10, Θ_{XPD}, F_{PB}, D_{X}, D_{Y}
Initialization:	Compute $\mathcal{E}_R$, Ω_{RC}, A_{SP}, κ_d. See Eqs. (E5), (E8), (E19), and (E18).
Step i:	Compute ζ using Eq. (E26).
Step ii:	Obtain $\hat{\zeta}$ by applying $f_{co}^{\mathrm{RL|CE}}(\zeta_{dB} \mid \Theta_{\mathrm{XPD}})$, using $\zeta_{dB} = 10\log_{10}\zeta_{CL}$ and Eq. (E25).
Step iii:	Convert $\hat{\zeta}$ into τ_{MIMO} using Eq. (E24).
Output:	τ_{MIMO}

E.3.2 Estimations in LDM Scenarios (Layered MIMO Type A)

This section illustrates Class E estimations for Layered MIMO Type A systems (see Annex O in [3] for Layered MIMO systems). τ_{MIMO}s for CL and EL are identified in the following subsections.

Note: Throughout this section, the parameters $\mathcal{E}_R$, Δ_{LDM}, A_{SP}, and κ_d conform to the definitions in the previous sections, referring to Eqs. (E5), (E8), (E19), and (E18).

Note: τ_{SISO} corresponds to the measurements obtained without applying LDM, and also pilot boosting.

E.3.2.1 Core Layer

The CL model is described below per channel condition. The notation $\tau_{MIMO}|_{LDM\ CL}$ indicates the τ_{MIMO} of CL as in Section E.2.2.

E.3.2.1.1 AWGN Channel

The C/N estimate is modeled as follows when $ChMod$ = AWGN:

$$\tau_{MIMO}|_{LDM\ CL} = \frac{\zeta}{\kappa_d} = \frac{\mathcal{E}_R\Delta_{LDM} - 1 + \sqrt{(\mathcal{E}_R\Delta_{LDM} - 1)^2 + \Omega_{\mathrm{AWGN}}(1 - \mathcal{E}_R\Delta_{LDM}^2)(\mathcal{E}_R - 1)}}{\Omega_{\mathrm{AWGN}}(1 - \mathcal{E}_R\Delta_{LDM}^2)\kappa_d}, \quad \text{Eq. (E28)}$$

where $\Omega_{\mathrm{AWGN}} = (2\rho_L - 1)^2$.

The estimation procedure computing $\tau_{MIMO}|_{LDM\ CL}$ unfolds as follows:

Input:	τ_{SISO}, $ChMod$ = AWGN, Θ_{XPD}, F_{PB}, D_{X}, D_{Y}, IL
Initialization:	Compute $\mathcal{E}_R$, Ω_{AWGN}, A_{SP}, κ_d, and Δ_{LDM}.
Step i:	Compute Eq. (E28) to obtain $\tau_{MIMO}|_{LDM\ CL}$: Calculate ζ and divide it by κ_d.
Output:	$\tau_{MIMO}|_{LDM\ CL}$

E.3.2.1.2 Rayleigh Channel

When conditioned on RL channel, $\tau_{MIMO}|_{LDM\ CL}$ is described as

$$\tau_{MIMO}|_{LDM\ CL} = \frac{(A_{SP}^2 + \kappa_d)\zeta_r + \sqrt{\left((A_{SP}^2 + \kappa_d)\zeta_r\right)^2 + 4A_{SP}^2\kappa_d\zeta_r}}{2A_{SP}^2\kappa_d}, \quad \text{Eq. (E29)}$$

where

$$\zeta_r = \frac{\hat{\zeta}_{CL}}{1 - \Delta_{LDM} - \Delta_{LDM}\hat{\zeta}_{CL}} \quad \text{Eq. (E30)}$$

traces back to

$$\hat{\zeta}_{CL} = \zeta_{CL} \times 10^{\frac{f_{co}^{\mathrm{RL|CE}}(\zeta_{CL}^{dB} \mid \Theta_{\mathrm{XPD}})}{10}}. \quad \text{Eq. (E31)}$$

This metric $\hat{\zeta}_{CL}$ is factorized into

$$\zeta_{CL} = \frac{(1-\Delta_{LDM})\zeta}{1+\Delta_{LDM}\zeta} \qquad \text{Eq. (E32)}$$

and $f_{co}^{\mathrm{RL|CE}}\left(\zeta_{CL}^{dB} \mid \Theta_{\mathrm{XPD}}\right)$ as described above. Note that the same $f_{co}^{\mathrm{RL|CE}}(\cdot)$ as in Section E.3.1.2 shall be used while holding $\zeta_{CL}^{dB} = 10\log_{10}\zeta_{CL}$ as input.

The intermediate estimate ζ is given by

$$\zeta = \frac{\mathcal{E}_R\Delta_{LDM} - 1 + \sqrt{(\mathcal{E}_R\Delta_{LDM}-1)^2 + \Omega_{\mathrm{RL}}(1-\mathcal{E}_R\Delta_{LDM}^2)(\mathcal{E}_R - 1)}}{\Omega_{\mathrm{RL}}(1-\mathcal{E}_R\Delta_{LDM}^2)} \qquad \text{Eq. (E33)}$$

where $\Omega_{\mathrm{RL}} = {\rho_N}^2 + (1-\rho_N)^2$ shares the same definition as in Section E.3.1.2.

The estimation procedure computing $\tau_{MIMO}|_{LDM\ CL}$ unfolds as follows:

Input:	τ_{SISO}, $ChMod$ = RL, Θ_{XPD}, F_{PB}, D_{X}, D_{Y}, IL
Initialization:	Compute $\mathcal{E}_R$, Ω_{RL}, A_{SP}, κ_d, and Δ_{LDM}.
Step i:	Compute ζ using Eq. (E33).
Step ii:	Convert ζ into ζ_{CL}. See Eq. (E32).
Step iii:	Obtain $\hat{\zeta}_{CL}$ by applying $f_{co}^{\mathrm{RL|CE}}\left(\zeta_{CL}^{dB} \mid \Theta_{\mathrm{XPD}}\right)$, using $\zeta_{CL}^{dB} = 10\log_{10}\zeta_{CL}$ and Eq. (E31).
Step iv:	Convert $\hat{\zeta}_{CL}$ into ζ_r using Eq. (E30).
Step v:	Obtain $\tau_{MIMO}|_{LDM\ CL}$ from Eq. (E29).
Output:	$\tau_{MIMO}|_{LDM\ CL}$

E.3.2.1.3 Rician Channel

When conditioned on RC channel, $\tau_{MIMO}|_{LDM\ CL}$ is described as

$$\tau_{MIMO}|_{LDM\ CL} = \frac{(A_{SP}^2+\kappa_d)\zeta_r - (1+K)\kappa_d + \sqrt{\left((A_{SP}^2+\kappa_d)\zeta_r - (1+K)\kappa_d\right)^2 + 4A_{SP}^2\kappa_d(1+K)\zeta_r}}{2A_{SP}^2\kappa_d} \qquad \text{Eq. (E34)}$$

where

$$\zeta_r = \frac{\hat{\zeta}_{CL}}{1-\Delta_{LDM}-\Delta_{LDM}\hat{\zeta}_{CL}} \qquad \text{Eq. (E35)}$$

traces back to

$$\hat{\zeta}_{CL} = \zeta_{CL} \times 10^{\frac{f_{co}^{\mathrm{RC|CE}}\left(\zeta_{CL}^{dB} \mid \Theta_{\mathrm{XPD}}\right)}{10}}. \qquad \text{Eq. (E36)}$$

This metric $\hat{\zeta}_{CL}$ is factorized into

$$\zeta_{CL} = \frac{(1-\Delta_{LDM})\zeta}{1+\Delta_{LDM}\zeta} \qquad \text{Eq. (E37)}$$

and $f_{co}^{\mathrm{RC|CE}}\left(\zeta_{CL}^{dB} \mid \Theta_{\mathrm{XPD}}\right)$ as described above. Note that the same $f_{co}^{\mathrm{RC|CE}}(\cdot)$ as in Section E.3.1.3 shall be used while holding $\zeta_{CL}^{dB} = 10\log_{10}\zeta_{CL}$ as input.

The intermediate estimate ζ is given by

$$\zeta = \frac{\mathcal{E}_R\Delta_{LDM} - 1 + \sqrt{(\mathcal{E}_R\Delta_{LDM} - 1)^2 + \Omega_{\mathrm{RL}}(1 - \mathcal{E}_R\Delta_{LDM}^2)(\mathcal{E}_R - 1)}}{\Omega_{\mathrm{RL}}(1 - \mathcal{E}_R\Delta_{LDM}^2)} \qquad \text{Eq. (E38)}$$

where Ω_{RC} agrees with the same definition as in Section E.2.1.3.

The estimation procedure computing $\tau_{MIMO}|_{LDM\ CL}$ unfolds as follows:

Input:	τ_{SISO}, $ChMod$ = RC, Θ_{XPD}, F_{PB}, D_{X}, D_{Y}, IL
Initialization:	Calculate $\mathcal{E}_R$, Ω_{RC}, A_{SP}, κ_d, and Δ_{LDM}.
Step i:	Calculate ζ using Eq. (E38).
Step ii:	Convert ζ into ζ_{CL}. See Eq. (E37).
Step iii:	Obtain $\hat{\zeta}_{CL}$ by applying $f_{co}^{\mathrm{RC|CE}}\left(\zeta_{CL}^{dB} \mid \Theta_{\mathrm{XPD}}\right)$, using $\zeta_{CL}^{dB} = 10\log_{10}\zeta_{CL}$ and Eq. (E36).
Step iv:	Convert $\hat{\zeta}_{CL}$ into ζ_r using Eq. (E35).
Step v:	Obtain $\tau_{MIMO}|_{LDM\ CL}$ from Eq. (E34)
Output:	$\tau_{MIMO}|_{LDM\ CL}$

E.3.2.2 Enhanced Layer

When $\tau_{MIMO}|_{LDM\ EL}$ designates the τ_{MIMO} of EL as in Section E.2.2, it is described per channel condition as

$$\tau_{\mathrm{MIMO}}|_{\mathrm{LDM\ EL}} = \begin{cases} \tau_{\mathrm{MIMO}}|_{EL}^{\mathrm{AWGN}} & ChMod = \mathrm{AWGN} \\ \tau_{\mathrm{MIMO}}|_{EL}^{\mathrm{RL}} & ChMod = \mathrm{RL} \\ \tau_{\mathrm{MIMO}}|_{EL}^{\mathrm{RC}} & ChMod = \mathrm{RC} \end{cases} \qquad \text{Eq. (E39)}$$

where:

$$\tau_{\mathrm{MIMO}}|_{EL}^{\mathrm{AWGN}} = \frac{\zeta_{EL}}{\kappa_d}$$

$$\tau_{\mathrm{MIMO}}|_{EL}^{\mathrm{RL}} = \frac{(A_{SP}^2 + \kappa_d)\zeta_{EL} + \sqrt{\left((A_{SP}^2 + \kappa_d)\zeta_{EL}\right)^2 + 4A_{SP}^2\kappa_d\zeta_{EL}}}{2A_{SP}^2\kappa_d}$$

$$\tau_{\mathrm{MIMO}}|_{EL}^{\mathrm{RC}} = \frac{(A_{SP}^2 + \kappa_d)\zeta_{EL} - (1+K)\kappa_d + \sqrt{\left((A_{SP}^2 + \kappa_d)\zeta_{EL} - (1+K)\kappa_d\right)^2 + 4A_{SP}^2\kappa_d(1+K)\zeta_{EL}}}{2A_{SP}^2\kappa_d}$$

specify the respective realizations. All those realization instances trace back to an intermediate estimate

$$\zeta_{EL} = \frac{\zeta}{\Delta_{LDM}} \times 10^{\frac{f_{co}^{ChMod|\mathrm{CE}}(\zeta_{dB} \mid \Theta_{\mathrm{XPD}})}{10}},$$

which attributes to

$$\zeta = \frac{-1 + \sqrt{1 + \Omega_{ChMod}(\mathcal{E}_R - 1)}}{\Omega_{ChMod}},$$

Δ_{LDM}, and $f_{co}^{ChMod|\mathrm{CE}}(\zeta_{dB} \mid \Theta_{\mathrm{XPD}})$. Note that $f_{co}^{ChMod|\mathrm{CE}}(\cdot)$ herein agrees with the same described in Section E.3.1 for each $ChMod$ realization. Ω_{ChMod} refers to Eqs. (E7), (E8), and (E10).

Note: The estimation for LDM EL overall resembles that for non-LDM case in Section E.3.1 but involves a scaling of ζ by $1/\Delta_{LDM}$ during the process.

The estimation procedure computing $\tau_{MIMO}|_{LDM\ EL}$ unfolds as follows:

Input:	τ_{SISO}, $ChMod$, Θ_{XPD}, F_{PB}, D_{X}, D_{Y}, IL
Initialization:	Calculate $\mathcal{E}_R$, Ω_{ChMod}, A_{SP}, κ_d, and Δ_{LDM}.
Step i:	Calculate ζ according to $ChMod$. See Eq. (E4).
Step ii:	Convert ζ into ζ_{EL}, using $f_{co}^{ChMod|\mathrm{CE}}\left(\zeta_{CL}^{dB} \mid \Theta_{\mathrm{XPD}}\right)$ and Δ_{LDM}.
Step iii:	Obtain $\tau_{MIMO}|_{LDM\ EL}$ from ζ_{EL}, using Eq. (E39).
Output:	$\tau_{MIMO}|_{LDM\ EL}$

E.3.3 Calculation Examples

Example calculations are given below assuming:

τ_{SISO}	1.9588 (= 2.92 dB)
$ChMod$	RL
Θ_{XPD}	$\mathrm{XPD_N}$ = 10 dB ($\mathrm{XPD_L}$ = N/A)
F_{PB}	5.3 dB
D_{X}	8
D_{Y}	2

Note: This parameter setting refers to a ModCod combination described in Table E.2.5, MP8_2 pilot pattern, and **L1D_scattered_pilot_boost** with value 100.

Based on input parameters above, the initialization step prepares parameters computed as:

$$\mathcal{E}_R = 1 + 2 \times 1.9588 + (1.9588)^2 = 8.7548$$

$$\rho_N = 10^{\frac{10}{10}}/(1 + 10^{\frac{10}{10}}) = 0.9091$$

$$\Omega_{\mathrm{RL}} = (0.9091)^2 + (1 - 0.9091)^2 = 0.8347$$

$$A_{SP} = 10^{\frac{5.3}{20}} = 1.8408$$

$$\kappa_d = 1/\left(1 - \frac{1}{8\times 2} + \frac{1.8408^2}{8\times 2}\right) = 0.8701$$

These parameter values are uniformly applied to both non-LDM and LDM examples that follow.

E.3.3.1 Non-LDM Example

Based on the parameter set described above, Class E estimation for non-LDM configuration proceeds as follows.

ζ and ζ_{dB} are computed as:

$$\zeta = \frac{\left(-1 + \sqrt{1 + 0.8347 \times (8.7548 - 1)}\right)}{0.8347} = 2.0770$$

$$\zeta_{dB} = 10 \log_{10} 2.0770 = 3.1743$$

$f_{co}^{\mathrm{RL|CE}}(\zeta_{dB} \mid \Theta_{\mathrm{XPD}})$ is computed as:

$$\begin{aligned} f_{co}^{\mathrm{RL|CE}}(3.1743 \mid \mathrm{XPD_N} = 10\ \mathrm{dB}) = & -1.6 \times 10^{-7} \times (3.1743)^5 + 1.485 \times 10^{-5} \times (3.1743)^4 \\ & - 4.469 \times 10^{-4} \times (3.1743)^3 + 2.345 \times 10^{-3} \times (3.1743)^2 + \\ & 0.1149 \times (3.1743) + 0.7823 \\ & = 1.1578 \end{aligned}$$

$\hat{\zeta}$ is computed as:

$$\hat{\zeta} = 2.0770 \times 10^{\frac{1.1578}{10}} = 2.7115$$

The estimate τ_{MIMO} is then derived as

$$\tau_{MIMO} = \frac{(1.8408^2+0.8701)\times 2.7115+\sqrt{\left((1.8408^2+0.8701)\times 2.7115\right)^2+4\times 1.8408^2\times 0.8701\times 2.7115}}{2\times 1.8408^2\times 0.8701} = 4.1387$$

and leads to the dB scale estimate

$$10 \log_{10} \tau_{MIMO} \qquad 6.1687\ \mathrm{dB}.$$

E.3.3.2 LDM Example

LDM examples are given below assuming:

IL 10 dB

The initialization step additionally prepares a parameter computed therefrom:

$$\Delta_{LDM} = 10^{-\frac{10}{10}}/(1 + 10^{-\frac{10}{10}}) = 0.0909$$

This LDM parameter value is uniformly applied to both CL and EL examples that follow.

E.3.3.2.1 Core Layer Example

ζ for CL is computed as:

$$\zeta = \frac{\left(8.7548\times 0.0909-1+\sqrt{(8.7548\times 0.0909-1)^2+0.8347\times(1-8.7548\times 0.0909^2)\times(8.7548-1)}\right)}{0.8347\times(1-8.7548\times 0.0909^2)} = 2.9120$$

ζ_{CL} and ζ_{CL}^{dB} are computed as:

$$\zeta_{CL} = \frac{(1-0.0909)\times 2.9120}{1+0.0909\times 2.9120} = 2.0932$$

$$\zeta_{CL}^{dB} = 10\log_{10} 2.0932 = 3.2080$$

$f_{co}^{\mathrm{RL|CE}}\left(\zeta_{CL}^{dB} \mid \Theta_{\mathrm{XPD}}\right)$ is computed as:

$$\begin{aligned} f_{co}^{\mathrm{RL|CE}}(3.2080 \mid \mathrm{XPD_N} = 10\ \mathrm{dB}) = & -1.6\times 10^{-7}\times(3.2080)^5 + 1.485\times 10^{-5}\times(3.2080)^4 \\ & -4.469\times 10^{-4}\times(3.2080)^3 + 2.345\times 10^{-3}\times(3.2080)^2 + \\ & 0.1149\times(3.2080) + 0.7823 \\ & = 1.1618 \end{aligned}$$

$\hat{\zeta}_{CL}$ is computed as:

$$\hat{\zeta}_{CL} = 2.0932\times 10^{\frac{1.1618}{10}} = 2.7352$$

ζ_r is computed as:

$$\zeta_r = \frac{2.7352}{1-0.0909-0.0909\times 2.7352} = 4.1414$$

The estimate $\tau_{MIMO}|_{LDM\ CL}$ is then derived as

$$\tau_{MIMO}|_{LDM\ CL} = \frac{(1.8408^2+0.8701)\times 4.1414+\sqrt{\left((1.8408^2+0.8701)\times 4.1414\right)^2+4\times 1.8408^2\times 0.8701\times 4.1414}}{2\times 1.8408^2\times 0.8701}$$
$$= 6.2081$$

and leads to the dB scale estimate

$$10\log_{10}\tau_{MIMO}|_{LDM\ CL} \qquad 7.9296\ \mathrm{dB}.$$

E.3.3.2.2 Enhanced Layer Example

ζ and ζ_{dB} for EL is computed as:

$$\zeta = \frac{\left(-1+\sqrt{1+0.8347\times(8.7548-1)}\right)}{0.8347} = 2.0770$$

$$\zeta_{dB} = 10\log_{10} 2.0770 = 3.1743$$

$f_{co}^{\mathrm{RL|CE}}(\zeta_{dB} \mid \Theta_{\mathrm{XPD}})$ is computed as:

$$\begin{aligned} f_{co}^{\mathrm{RL|CE}}(3.1743 \mid \mathrm{XPD_N} = 10\ \mathrm{dB}) = & -1.6\times 10^{-7}\times(3.1743)^5 + 1.485\times 10^{-5}\times(3.1743)^4 \\ & -4.469\times 10^{-4}\times(3.1743)^3 + 2.345\times 10^{-3}\times(3.1743)^2 + \end{aligned}$$

$$0.1149 \times (3.1743) + 0.7823$$
$$= 1.1578$$

ζ_{EL} is computed as:

$$\zeta_{EL} = \frac{2.0770}{0.0909} \times 10^{\frac{1.1578}{10}} = 29.827$$

The estimate $\tau_{MIMO}|_{LDM\ EL}$ is then derived as

$$\tau_{MIMO}|_{LDM\ EL} = \frac{(1.8408^2+0.8701)\times 29.827+\sqrt{\left((1.8408^2+0.8701)\times 29.827\right)^2+4\times 1.8408^2\times 0.8701\times 29.827}}{2\times 1.8408^2\times 0.8701}$$
$$= 43.315$$

and leads to the dB scale estimate

$$10\log_{10}\tau_{MIMO}|_{LDM\ CL} \qquad 16.366\ \text{dB}.$$

Add a new Annex F as follows:

Annex F: MIMO Channel Characterization

F.1 INTRODUCTION

This Annex provides a fundamental model describing MIMO channel environments. The presented is a stochastic model enabling abstraction of MIMO channel environment and supports theoretic estimations, analysis, and applications possible otherwise, such as those in Annex E. Channel distortions in this model apply to baseband cells and account for the small-scale fading effect and interactions between Polarization paths. There is a provision to support estimating Channel XPD from the respective properties of transmit and receive antenna units.

Note: The presented gives a mathematical rationale for MIMO channel model described in Section E.1.2. Reformulation of the model yields Table E.1.1, preserving equivalence. There also is a provision to support comprehension of field observations.

F.2 PRELIMINARIES AND SCOPE

F.2.1 General

ATSC 3.0 MIMO consists of two Polarization paths spatially multiplexed between them. A generic expression according to this configuration shapes the signal model as

$$\begin{bmatrix} y_0 \\ y_1 \end{bmatrix} = \mathbf{H} \begin{bmatrix} x_0 \\ x_1 \end{bmatrix} + \begin{bmatrix} n_0 \\ n_1 \end{bmatrix},$$

where:

y_0, y_1 denote the received signals in terms of baseband cells associated with respective Polarization chain;

x_0, x_1 denote the transmit signals in terms of baseband cells associated with respective Polarization chain;

n_0, n_1 denote additive noise observed at the baseband cell level, each affecting the respective Polarization chain;

and where the subscripts 0 and 1 indicate association with Polarization #1 and #2, respectively. This follows theoretic conventions using descriptions at the baseband cell level. The transmit cells x_0 and x_1 are assumed as i.i.d. unbiased complex Gaussian random variables unless otherwise noted.

The channel matrix $\mathbf{H}$ is described as

$$\mathbf{H} = \begin{bmatrix} h_{00} & h_{10} \\ h_{01} & h_{11} \end{bmatrix}. \qquad \text{Eq. (F)}$$

The diagonal elements represent co-polarization fading, while the off-diagonal elements denote cross-polarization counterparts. These off-diagonal entities quantify the contribution of signals with Polarization converted from their original orientation.

Channel XPD in this context characterizes the amount of isolation between co- and cross-polarization signals. This is described in terms of the relative ratios

$$10\log_{10}\left(\frac{\mathbb{E}[|h_{00}|^2]}{\mathbb{E}[|h_{10}|^2]}\right) \quad \text{and} \quad 10\log_{10}\left(\frac{\mathbb{E}[|h_{11}|^2]}{\mathbb{E}[|h_{01}|^2]}\right)$$

when expressed in dB scale. The operator $\mathbb{E}[\cdot]$ denotes expectation over ensembles. Symmetric channel is regarded unless otherwise noted, i.e., $\mathbb{E}[|h_{00}|^2] = \mathbb{E}[|h_{11}|^2]$ and $\mathbb{E}[|h_{10}|^2] = \mathbb{E}[|h_{01}|^2]$.

Each element in **H** can be split into LoS and NLoS components, each exhibiting distinct statistical properties. This Annex proceeds with a Rician model description that renders those LoS and NLoS components as additive. Channel XPDs for the LoS and NLoS components are individually defined accordingly, while the overall Channel XPD is specified in terms of Effective Channel XPD. Note that Annex E refers to this Rician model as a generalized formulation encompassing AWGN and Rayleigh models.

F.2.2 Antenna XPD and Channel XPD

Channel XPD is partially attributed to antenna impairments, which introduce cross-polarization leakage to radio signals. Polarized waves passing through antennas exhibit some degree of mixing in practice, whereas ideal antennas would ensure perfect isolation. The extent of this leakage (or isolation) is measured in terms of Antenna XPD.

This effect occurs at both transmit and receive antennas. Antenna XPDs for transmit and receive antennas are hence defined individually as $\mathrm{XPD}_{\mathrm{Tx}}^{\mathrm{Ant}}$ and $\mathrm{XPD}_{\mathrm{Rx}}^{\mathrm{Ant}}$ while sharing a common definition

$$10\log_{10}\left(\frac{\text{Co}-\text{polarized signal power at the antenna output}}{\text{Polarization}-\text{shifted signal power at the antenna output}}\right).$$

Note: The terminology in this Annex distinguishes between Antenna XPD and Channel XPD. Antenna XPD pertains to the input and output characteristics of individual antennas, while Channel XPD characterizes the overall channel incorporating Antenna XPDs' contribution. These semantic distinctions are detailed in Section F.2.5.

F.2.3 Reflection and Polarization Conversion

Wave reflections during the air propagation may accompany polarization conversion. Scatters may introduce an unexpected increase in Channel XPD thereby. Such random effect is parameterized in terms of the expected amount of polarization shift, which can be statistically determined. This modeling applies exclusively to the NLoS channel component, as the LoS counterpart does not involve any signal bouncing.

The statistics of polarization conversion are assumed as symmetric between the two Polarization orientations, unless otherwise noted as in Section F.3.3.

F.2.4 Scope

The scope of this Annex includes:

- Channel modeling for ATSC 3.0 MIMO systems that reflects inter-polarization interactions attributed to antenna properties and physics-driven factors observable in fields.
- Comprehension of underlying factors related.

- Evaluation of Channel XPD derived therefrom.

F.2.5 Terms and Notation

Terms used in this Annex are enumerated as follows:

Channel XPD – The XPD defined at the input and output of MIMO channels, in an inclusive context that encompasses contributions from fading and antenna. When the channel includes both LoS and NLoS components, Channel XPDs specific to these channel components can be defined individually.

Antenna XPD – The XPD defined at the input and output of an individual antenna.

Effective Channel XPD – The Channel XPD explicitly indicating the value measured over the entire channel, combining the contributions of LoS and NLoS components.

Parameter notations used in this Annex are enumerated as follows:

$\mathrm{XPD_L}$ denotes a dB scale Channel XPD evaluated in the LoS part of MIMO channel;

$\mathrm{XPD_N}$ denotes a dB scale Channel XPD evaluated in the NLoS part of MIMO channel;

$\mathrm{XPD_{eff}}$ denotes an Effective Channel XPD measured in dB scale;

$\mathrm{XPD_{Tx}^{Ant}}$ denotes a dB scale Antenna XPD measured at the transmit antenna;

$\mathrm{XPD_{Rx}^{Ant}}$ denotes a dB scale Antenna XPD measured at the receive antenna;

χ_{LoS} is the linear scale expression of $\mathrm{XPD_L}$, i.e., $\chi_{LoS} = 10^{\frac{XPD_L}{10}}$;

χ_{NLoS} is the linear scale expression of $\mathrm{XPD_L}$, i.e., $\chi_{LoS} = 10^{\frac{XPD_N}{10}}$;

χ_{eff} is the linear scale expression of $\mathrm{XPD_{eff}}$, i.e., $\chi_{LoS} = 10^{\frac{XPD_{eff}}{10}}$;

e_T denotes the relative level of cross-polarization leakage compared to co-polarization signal power within the radiation output of transmit antenna. This value is determined by $\mathrm{XPD_{Tx}^{Ant}}$ and is expressed in linear scale;

e_R denotes the relative level of cross-polarization leakage compared to co-polarization signal power within the radiation output of transmit antenna. This value is determined by $\mathrm{XPD_{Tx}^{Ant}}$ and is expressed in linear scale;

r $\in [0, 1]$ denotes the fraction of polarization-shifted signal power within the reflected signal waves;

ρ_L $\in [0, 1]$ denotes a parameter representing the power distribution between co- and cross-polarization components in the LoS part of the channel model. This value is determined by $\mathrm{XPD_L}$;

ρ_N $\in [0, 1]$ denotes a parameter representing the power distribution between of co- and cross-polarization components in the NLoS part of the channel model. This value is determined by $\mathrm{XPD_N}$;

K is the Rician K-factor.

F.3 MODEL DESCRIPTION

$\mathrm{XPD_{Tx}^{Ant}}$ and $\mathrm{XPD_{Rx}^{Ant}}$ applies to the model as

$$\mathbf{H} = \begin{bmatrix} 1 & \sqrt{e_R} \\ \sqrt{e_R} & 1 \end{bmatrix} (A_L \mathbf{G}_{LoS} + A_N \mathbf{G}_{NLoS}) \begin{bmatrix} 1 & \sqrt{e_T} \\ \sqrt{e_T} & 1 \end{bmatrix} \triangleq A_L \mathbf{H}_L^o + A_N \mathbf{H}_N^o$$

where $e_R = 10^{-\frac{\mathrm{XPD}_{\mathrm{Rx}}^{\mathrm{Ant}}}{10}}$ and $e_T = 10^{-\frac{\mathrm{XPD}_{\mathrm{Tx}}^{\mathrm{Ant}}}{10}}$ realize cross-polarization leakage at the antennas; and A_L and A_N are scaling coefficients that normalize and weight the LoS and NLoS contributions. The parameters A_L and A_N do not require explicit specification since they are implicitly accounted for in the Rician K-factor within the final model formulation.

$\mathbf{H}_L^o$ and $\mathbf{H}_N^o$ denote the primitive forms of LoS and NLoS components that are expressed as

$$\mathbf{H}_L^o = \begin{bmatrix} 1 & \sqrt{e_R} \\ \sqrt{e_R} & 1 \end{bmatrix} \mathbf{G}_{LoS} \begin{bmatrix} 1 & \sqrt{e_T} \\ \sqrt{e_T} & 1 \end{bmatrix}$$

and

$$\mathbf{H}_N^o = \begin{bmatrix} 1 & \sqrt{e_R} \\ \sqrt{e_R} & 1 \end{bmatrix} \mathbf{G}_{NLoS} \begin{bmatrix} 1 & \sqrt{e_T} \\ \sqrt{e_T} & 1 \end{bmatrix}.$$

The propagation fading terms $\mathbf{G}_{LoS}$ and $\mathbf{G}_{NLoS}$ therein are defined as

$$\mathbf{G}_{LoS} = \begin{bmatrix} 1 & 0 \\ 0 & 1 \end{bmatrix}$$

and

$$\mathbf{G}_{NLoS} = \begin{bmatrix} \sqrt{(1-r)}g_{00}^N & \sqrt{r}g_{10}^N \\ \sqrt{r}g_{01}^N & \sqrt{(1-r)}g_{11}^N \end{bmatrix},$$

where:

g_{00}^N, g_{10}^N, g_{01}^N, g_{11}^N denote the normalized random fading gain that apply to each entry of $\mathbf{G}_{NLoS}$, which are i.i.d. complex Gaussian random variables with a zero-mean and unit variance.

Abstraction and normalization reformulate the channel model to be

$$\mathbf{H} = \sqrt{\frac{K}{1+K}}\mathbf{H}_{AWGN} + \sqrt{\frac{1}{1+K}}\mathbf{H}_{RL}$$

that agrees with Table E.1.1 in Annex E. The LoS and NLoS components herein are specified as

$$\mathbf{H}_{AWGN} = \begin{bmatrix} \sqrt{\rho_L} & \sqrt{1-\rho_L} \\ \sqrt{1-\rho_L} & \sqrt{\rho_L} \end{bmatrix} \quad \text{and} \quad \mathbf{H}_{RL} = \begin{bmatrix} \sqrt{\rho_N}g_{00} & \sqrt{1-\rho_N}g_{10} \\ \sqrt{1-\rho_N}g_{01} & \sqrt{\rho_N}g_{11} \end{bmatrix},$$

where:

g_{00}, g_{10}, g_{01}, g_{11} denote the normalized random fading gain that apply to each entry of $\mathbf{H}_{RL}$, which are i.i.d. complex Gaussian random variables with a zero-mean and unit variance.

ρ_L and ρ_N comply with the following equations determined by e_T, e_R, and r:

$$\rho_L = \frac{\chi_{LoS}}{1+\chi_{LoS}}, \qquad \rho_N = \frac{\chi_{NLoS}}{1+\chi_{NLoS}},$$

and are used on behalf of Channel XPD values.

The Channel XPD values are specified as

$$\chi_{LoS} = \left(\frac{1+\sqrt{e_R e_T}}{\sqrt{e_R}+\sqrt{e_T}}\right)^2$$

and

$$\chi_{NLoS} = \frac{1+e_R e_T-(1-e_R-e_T+e_R e_T)r}{e_R+e_T+(1-e_R-e_T+e_R e_T)r},$$

where these are the linear scale expressions of $\mathrm{XPD_L} = 10\log_{10}\chi_{LoS}$ and $\mathrm{XPD_N} = 10\log_{10}\chi_{NLoS}$.

Effective Channel XPD combining χ_{LoS} and χ_{NLoS} amounts to

$$\chi_{eff} = \frac{K(1+\sqrt{e_R e_T})^2+1+e_R e_T-(1-e_R-e_T+e_R e_T)r}{K(\sqrt{e_R}+\sqrt{e_T})^2+e_R+e_T+(1-e_R-e_T+e_R e_T)r},$$

whose dB scale expression finds $\mathrm{XPD_{eff}} = 10\log_{10}\chi_{eff}$.

Note: This Effective Channel XPD is the value likely to be measured at field receivers. Most receivers are unable to distinguish between LoS and NLoS contributions. Such receiver implementations will limit the measurement ability to the comprehensive value of Effective Channel XPD rather than detailed evaluations for $\mathrm{XPD_L}$ and $\mathrm{XPD_N}$.

F.3.1 Special Case: AWGN Channel

AWGN channel designates a special case with $K \to \infty$. NLoS signals are absent in AWGN channel and $\mathbf{G}_{NLoS}$ is zero accordingly. The Effective Channel XPD agrees with the XPD evaluated in the LoS part, i.e., $\chi_{eff} = \chi_{LoS}$. In this case, Effective Channel XPD across the overall channel elements is deterministic as controlled by the properties of transmit and receive antennas.

F.3.2 Special Case: Rayleigh Channel

Rayleigh channel designates a special case with $K = 0$. LoS signals are absent in Rayleigh channel and $\mathbf{G}_{LoS}$ is zero accordingly. The Effective Channel XPD agrees with the XPD evaluated in the NLoS part, i.e., $\chi_{eff} = \chi_{NLoS}$. In this case, uncontrollable environmental factor r affects the Effective Channel XPD in addition to antenna properties.

F.3.3 Generalization Toward Asymmetric Reflection Effects

Field observations may advocate channel asymmetricity in that XPD deviates between Polarizations. Such asymmetry is mostly ascribed to physical reactions in radio wave reflections: The energy loss and Polarization shift may not amount alike between horizontal and vertical polarizations. Those may depend on the orientation of the reflection plane as well.

The NLoS channel component can be adjusted to accommodate generalization as

$$\mathbf{G}_{NLoS} = \begin{bmatrix} \sqrt{2b_G(1-r_0)}g_{00}^N & \sqrt{2(1-b_G)r_1}g_{10}^N \\ \sqrt{2b_G r_0}g_{01}^N & \sqrt{2(1-b_G)(1-r_1)}g_{11}^N \end{bmatrix}$$

where:

$b_G \in [0,1]$ denotes the relative weight of energy from Polarization #1 retained after reflections compared to that of Polarization #2;

r_0 denotes the portion of signal power converted from Polarization #1 to Polarization #2, relative to the total reflected signal power originating from Polarization #1 incidence;

r_1 denotes the portion of signal power converted from Polarization #2 to Polarization #1, relative to the total reflected signal power originating from Polarization #2 incidence.

In this generalized model, XPD_N and XPD_{eff} are split based on the Polarization orientation in which they are measured. The XPD_N values measured on Polarizations #1 and #2 are denoted as $XPD_N(0)$ and $XPD_N(1)$, respectively, and are defined as $\mathrm{XPD_N}(0) = 10\log_{10}\chi_{NLoS}(0)$ and $\mathrm{XPD_N}(1) = 10\log_{10}\chi_{NLoS}(1)$ for

$$\chi_{NLoS}(0) = \frac{b_G(1-r_0) + b_G r_0 e_R + (1-b_G)r_1 e_T + (1-b_G)(1-r_1)e_R e_T}{(1-b_G)r_1 + (1-b_G)(1-r_1)e_R + b_G(1-r_0)e_T + b_G r_0 e_R e_T}$$

and

$$\chi_{NLoS}(1) = \frac{b_G r_0 + (1-b_G)r_1 e_R + (1-b_G)(1-r_1)e_T + (1-b_G)r_1 e_R e_T}{(1-b_G)(1-r_1) + (1-b_G)r_1 e_R + b_G r_0 e_T + b_G(1-r_0)e_R e_T}.$$

The XPD_{eff} values measured on Polarizations #1 and #2 are denoted as $XPD_{eff}(0)$ and $XPD_{eff}(1)$ alike, and are specified by $\mathrm{XPD_{eff}}(0) = 10\log_{10}\chi_{eff}(0)$ and $\mathrm{XPD_{eff}}(1) = 10\log_{10}\chi_{eff}(1)$ for

$$\chi_{eff}(0) = \frac{K(1+\sqrt{e_R e_T})^2 + b_G(1-r_0) + b_G r_0 e_R + (1-b_G)r_1 e_T + (1-b_G)(1-r_1)e_R e_T}{K(\sqrt{e_R}+\sqrt{e_T})^2 + (1-b_G)r_1 + (1-b_G)(1-r_1)e_R + b_G(1-r_0)e_T + b_G r_0 e_R e_T}$$

and

$$\chi_{eff}(1) = \frac{K(1+\sqrt{e_R e_T})^2 + b_G r_0 + (1-b_G)r_1 e_R + (1-b_G)(1-r_1)e_T + (1-b_G)r_1 e_R e_T}{K(\sqrt{e_R}+\sqrt{e_T})^2 + (1-b_G)(1-r_1) + (1-b_G)r_1 e_R + b_G r_0 e_T + b_G(1-r_0)e_R e_T}.$$

Within $\mathbf{H} = \sqrt{\frac{K}{1+K}}\mathbf{H}_{AWGN} + \sqrt{\frac{1}{1+K}}\mathbf{H}_{RL}$ characterizing the overall channel, $\mathbf{H}_{RL}$ is modified accordingly as

$$\mathbf{H}_{RL} = \begin{bmatrix} \sqrt{2b_H\rho_N(0)}g_{00} & \sqrt{2b_H(1-\rho_N(0))}g_{10} \\ \sqrt{2(1-b_H)(1-\rho_N(1))}g_{01} & \sqrt{2(1-b_H)\rho_N(1)}g_{11} \end{bmatrix}$$

while $\mathbf{H}_{AWGN}$ remains the same as before. The parameters related refer to:

$\rho_N(0)$ denotes the power portion of co- and cross-polarization components originated in Polarization #1 signals, particularly in context of the NLoS part of MIMO channel. This value is determined by $\rho_N(0) = \frac{\chi_{NLoS}(0)}{1+\chi_{NLoS}(0)}$;

$\rho_N(1)$ denotes the power portion of co- and cross-polarization components originated in Polarization #2 signals, particularly in context of the NLoS part of MIMO channel. This value is determined by $\rho_N(1) = \frac{\chi_{NLoS}(1)}{1+\chi_{NLoS}(1)}$;

b_H $\in$ $[0, 1]$ denotes the relative weight of Polarization #1's signal energy observed at the receiver, compared to that of Polarization #2.

Note that b_H illustrates potential power asymmetricity between signal waves received through different Polarization orientations. This value is determined as

$$b_H = \frac{b_G(1-r_0) + (1-b_G)r_1 + \{b_G r_0 + (1-b_G)(1-r_1)\}e_R + \{(1-b_G)r_1 + b_G(1-r_0)\}e_T + \{(1-b_G)(1-r_1) + b_G r_0\}e_R e_T}{(1+e_R)(1+e_T)}.$$

F.4 CALCULATION EXAMPLE

Calculation exercise is introduced to instruct practices. This exercise applies an example parameter set of:

$\mathrm{XPD}_{\mathrm{Tx}}^{\mathrm{Ant}}$ 26 dB

$\mathrm{XPD}_{\mathrm{Rx}}^{\mathrm{Ant}}$ 26 dB

r 0.1 (= 10%)

Based on the given setting, model parameters are computed as follows. The given values of $\mathrm{XPD}_{\mathrm{Tx}}^{\mathrm{Ant}}$ and $\mathrm{XPD}_{\mathrm{Rx}}^{\mathrm{Ant}}$ transform into:

$$e_T = 10^{-\frac{26}{10}} = 2.5119 \times 10^{-3}$$

$$e_R = 10^{-\frac{26}{10}} = 2.5119 \times 10^{-3}$$

A combination of e_T, e_R, and r results in

$$\chi_{LoS} = \left(\frac{1 + \sqrt{(2.5119 \times 10^{-3}) \times (2.5119 \times 10^{-3})}}{\sqrt{2.5119 \times 10^{-3}} + \sqrt{2.5119 \times 10^{-3}}}\right)^2 = 100.03$$

$$\chi_{NLoS} = \frac{1+\left(2.5119\times10^{-3}\right)^2-\left(1-2.5119\times10^{-3}-2.5119\times10^{-3}+\left(2.5119\times10^{-3}\right)^2\right)\times0.1}{2.5119\times10^{-3}+2.5119\times10^{-3}+(1-2.5119\times10^{-3}-2.5119\times10^{-3}+(2.5119\times10^{-3})^2)\times0.1} = 8.1655$$

which coincide with

$\mathrm{XPD_L} = 10\log_{10} 100.03 = 20$ dB

$\mathrm{XPD_N} = 10\log_{10} 8.1655 = 9.35$ dB

When K = 10, Effective Channel XPD is computed as:

$$\chi_{eff} = \frac{10\times\left(1+\sqrt{(2.5119\times10^{-3})^2}\right)^2+1+\left(2.5119\times10^{-3}\right)^2-\left(1-2\times2.5119\times10^{-3}+\left(2.5119\times10^{-3}\right)^2\right)\times0.1}{10\times\left(2\times\sqrt{2.5119\times10^{-3}}\right)^2+2\times2.5119\times10^{-3}+(1-2.5119\times10^{-3}-2.5119\times10^{-3}+(2.5119\times10^{-3})^2)\times0.1} = 53.419$$

$$\mathrm{XPD_{eff}} = 10\log_{10} 53.419 = 17.28\ \mathrm{dB}$$

When K approaches infinity (AWGN channel), Effective Channel XPD is computed as:

χ_{eff} 100.03

$\mathrm{XPD_{eff}}$ 20 dB

When $K = 0$ (Rayleigh channel), Effective Channel XPD is computed as:

χ_{eff} 8.1655

$\mathrm{XPD_{eff}}$ 9.35 dB

Following values of ρ_L and ρ_N derived according to χ_{LoS} and χ_{NLoS} determine $\mathbf{H}_{AWGN}$ and $\mathbf{H}_{RL}$:

$$\rho_L = \frac{100.03}{1+100.03} = 0.9901$$

$$\rho_N = \frac{8.1655}{1+8.1655} = 0.8960$$

In conjunction with K, the overall channel model $\mathbf{H} = \sqrt{\frac{K}{1+K}}\mathbf{H}_{AWGN} + \sqrt{\frac{1}{1+K}}\mathbf{H}_{RL}$ is determined.

– End of Document –